**UNIVERSITÀ DEGLI STUDI DI NAPOLI FEDERICO II**

**DOTTORATO DI RICERCA IN**

**MEDICINA CLINICA E SPERIMENTALE**

*CURRICULUM IN SVILUPPO E ACCRESCIMENTO DELL'UOMO*

**XXIX Ciclo**

**Coordinatore: Prof. Gianni Marone**

**TESI DI DOTTORATO**

# STUDY OF PATHOPHYSIOLOGY OF POMPE DISEASE AND IDENTIFICATION OF NOVEL THERAPEUTIC TARGETS AND BIOMARKERS


TUTOR/RELATORE

**Chiar.mo**
**Prof. Giancarlo Parenti**

CANDIDATA

**Dott. Marcella Coletta**

# Summary

## GENERAL INTRODUCTION

- **Pompe disease**

Pompe disease (PD, glycogen storage disease type II) is a metabolic myopathy caused by mutations of the *GAA* gene and by functional deficiency of the acid alpha-glucosidase (GAA, acid maltase), a glycoside hydrolase involved in the lysosomal breakdown of glycogen [1]. The lack of functional GAA results in extensive glycogen storage in multiple tissues and massive accumulation of autophagic vesicles and autophagic debris in muscles [2].

The *GAA* gene, localized in 17q25.2-q25.3, consists of 20 exons spread over 28 kb of genomic sequence and encodes a protein of 952 amino acids with a predicted molecular mass of 110 kDa [3]. The 110 kDa GAA protein synthesized in the endoplasmic reticulum is a precursor polypeptide, which undergoes N-glycan processing in the Golgi apparatus, and is proteolytically processed in the lysosomes into active isoforms of 76 and 70 kDa, through an intermediate molecular form of 95 kDa [4]. In lysosome, the mature enzyme hydrolyzes the α-1,4 and 1,6-glycosidic bonds of glycogen, releasing glucose units that are then transported across the lysosomal membrane by a specific carrier [5].

Being GAA deficiency ubiquitous in PD, glycogen storage occurs in almost every tissue and cell type. However, disease manifestations are predominantly related to muscle involvement and heart and skeletal muscle are the major sites of pathology.

Muscle pathology has been extensively studied by several approaches, including immuno-histochemical procedures (with a wide range of cellular markers), and electron microscopy (***Fig. 1***). Muscle fibers show extensive vacuolization, with vacuoles containing glycogen particles, cytoplasmic debris, electron dense bodies, and multilamellar structures. Glycogen deposition may be seen also outside the vacuoles.

Particular interest has been recently paid to the presence of central accumulation of autophagic lipofuscin-like material [6]. In addition to these typical markers of PD pathology, other morphological changes have been described, such as the proliferation of the Golgi apparatus and abnormal caveolin expression [7, 8]. Despite the large number of studies, there are issues that remain unclear.

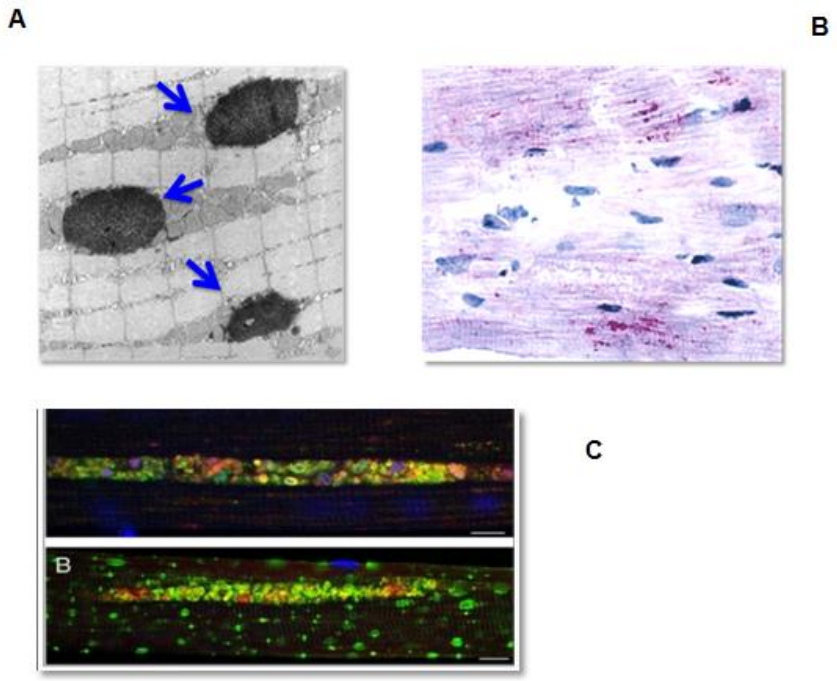


**Fig.1** (**A**) Electron microscopy: glycogen accumulation in PD muscle fibers. (**B**) PAS staining in PD muscle that shows glycogen accumulation. (**C**) PD muscle fibers show extensive vacuolization, with vacuoles containing glycogen particles and cytoplasmic debris.

So far more than 500 different *GAA* gene variations have been identified (The Human Gene Mutation Database, HGMD) and the type of mutation correlates in most cases with the residual enzyme activity. GAA activity may range from complete deficiency (<1%) in the severe forms, to partial (up to 30%) deficiency in milder forms. PD is often due to missense mutations in *GAA* gene that causes the synthesis of a misfolded enzyme protein.

Traditionally, PD patients have been classified into distinct categories, including an early onset “classical” form, early onset intermediate phenotypes, and the attenuated late onset juvenile and adult forms.

The “classic” infantile-onset form represents the severe end of this spectrum with a clearly defined phenotype, characterized by severe hypertrophic cardiomyopathy typical ECG pattern, generalized hypotonia and a rapidly progressive course. When untreated, classic infantile PD patients die by the end of the first year [9, 10].

In the late-onset, slowly progressive juvenile and adult-onset forms symptoms related to skeletal muscle dysfunction, resulting in both mobility and respiratory problems, are the primary manifestations [11]. The first symptoms usually start between the second and fourth decade and are in most instances related to impaired mobility and limb-girdle weakness. The age at onset, the rate of disease progression and the sequence of respiratory and skeletal muscle involvement vary substantially among different patients. The clinical variability makes diagnosis difficult and in several cases the final diagnosis is made many years after the start of symptoms.

Intermediate phenotypes (early onset without cardiomyopathy, childhood-onset) have also been described and characterized.

- **Therapy for Pompe disease: Enzyme replacement therapy**

The only approved treatment for PD is Enzyme replacement therapy (ERT) with recombinant human GAA (rhGAA). ERT is based on the concept that recombinant lysosomal hydrolases, in most cases enzyme precursors manufactured on large scale in eukaryotic cells systems (chinese hamster ovary cells), can be administered periodically to patients by an intravenous route. The enzymes are internalized by patients’ cells and tissues through the mannose or mannose-6-phosphate receptor pathways and are

ultimately delivered to lysosomes, where they are activated and replace the function of the defective hydrolases. The presence of mannose-6-phosphate ligands in the enzyme molecules and the integrity of the mannose-6-phosphate receptor pathway in the target cells and tissues are therefore crucial for the efficacy of this therapeutic approach.

In PD ERT showed remarkable success in reversing cardiac involvement in infantile-onset patient [12, 13, 14, 15, 16, 17]. Cardiac manifestations in most cases responded quickly and strikingly to ERT, with rapid regression of ventricular hypertrophy and near normalization of ventricular function.

However, limitations of ERT are becoming evident. First, not all patients respond equally well to treatment. Second, it is now clear that skeletal muscle (one of the major sites of disease and an important target of therapy) is more refractory to treatment than other tissues. Why this happens remains to be fully elucidated. It has been proposed that several factors concur in reducing the effectiveness of ERT in skeletal muscle. One of these factors is the preferential uptake of rhGAA by liver and the insufficient targeting of the enzyme to skeletal muscle [18]. The large mass of skeletal muscle and the relative deficiency of the mannose-6-phosphate receptors in muscle cells [19] also contribute to the poor correction of GAA activity.

Additional information derived from the studies performed in cultured fibroblasts from PD patients with different clinical forms showing abnormal cellular distribution of the CI-MPR [8]. These studies showed that mislocalization of the CI-MPR (the cation-independent mannose-6-phosphate receptor) resulted in less efficient internalization and lysosomal trafficking of rhGAA, mediated by this receptor. The degree of cellular abnormalities varied among the different cell lines and was correlated with the reduced uptake of rhGAA, indicating a possible mechanism for the variable response to ERT observed in different patients.

- **The pathophysiology of PD**

The role of secondary cellular events triggered by glycogen storage is now becoming a major field of investigation in PD. The spectrum of such abnormalities covers a wide range of events, including modulation of receptor responses and signal transduction cascades, activation of inflammatory responses, impaired intracellular trafficking of vesicles, membranes and membrane-bound proteins, impairment of autophagy, and others [20, 21].

Specifically, the derangement of autophagy is the most extensively studied and accurately characterized of these cellular abnormalities. Autophagy is a dynamic process involving the rearrangement of subcellular membranes to sequester cytoplasm and organelles in autophagic vesicles for delivery to lysosomes or vacuoles where the sequestered cargo is degraded and recycled [21]. For autophagy to accomplish its biological function (i.e. the turn-over of macromolecules and organelles), autophagic vesicles must fuse to lysosomes to form autophagolysosomes. When autophagy is blocked protein turn-over is impaired, causing the accumulation of ubiquitinated protein aggregates. In PD a number of studies demonstrated the massive accumulation of autophagic debris in the core of muscle fibers, decreased vesicular trafficking in cells, and an acidification defect in a subset of late endosomes/lysosomes [22, 23]. Why PD cells show an autophagic “build-up” and how these abnormalities contribute to muscle cell damage, however, remain to be fully elucidated. It is reasonable to speculate that further studies on the molecular mechanisms and cellular events elicited by glycogen storage will identify additional factors (i.e. oxidative stress, activation of genes responsible for the apoptotic cascade, etc) that may play a role in PD pathophysiology.

In addition to the abnormalities of autophagy, studies in PD fibroblasts demonstrated aberrant Golgi and trans-Golgi network morphology [8]. The abnormalities of the Golgi

apparatus were associated with changes in the distribution of CI-MPR, a membrane-bound protein mostly localized in these organelles. CI-MPR is sequestered in relatively inert vesicles deriving from the fusion of autophagosomes with substrate-engulfed lysosomes. An important consequence of the sequestration of CI-MPR in these organelles, is a depletion of functionally available CI-MPR at the plasma membrane. It is becoming clear that secondary cellular abnormalities may negatively affect the efficacy of the therapies currently available, thus providing clues to clarify the reasons for the variable response of different patients and tissues to therapies.

## AIM OF THE THESIS

While the genetics and the biochemistry of PD are well characterized, the molecular bases underlying the secondary cellular abnormalities are not clear. Several studies have been focused on abnormalities in the expression of the genes implicated in the control of housekeeping cellular functions. The general aim of my thesis is to improve the knowledge of PD pathophysiology and characterize pathways identifying novel targets for the treatment of PD, that may translate into improved efficacy of the ERT.

As I just mentioned, PD is characterized by different abnormalities in autophagy, in Golgi apparatus, in the CI-MPR distribution or in intracellular vesicular trafficking, so we thought it could be interesting to investigate also about the proteins interacting with GAA in normal condition and in PD. Secondary, we investigated about the other pathway that may be associated with autophagy abnormalities in a relationship of cause and effect. Among all molecular mechanisms, recently oxidative stress has been shown having a key role in autophagy regulation [24, 25]. In line with this evidence, the second aim of this work is to characterize the presence of ox-stress in PD and to investigate the possible role of ox-stress in ERT improvement.

Moreover, we have explored the potential of microRNAs (miRNAs) as new tool for understanding of the diseases pathophysiology and as new potential biomarkers to follow disease diagnosis, progression and follow up of patients. So far, there are several examples of alterations in the levels of circulating miRNAs associated with a disease condition.

## BIBLIOGRAPHY


[1] van der Ploeg AT, Reuser AJ (2008). Pompe's disease. *Lancet* **372**: 1342–1353.

[2] Shea L, Raben N (2009). Autophagy in skeletal muscle: implications for Pompe disease. Int J Clin Pharmacol Ther 47 Suppl 1: S42–47

[3] Hoefsloot LH, Hoogeveen-Westerveld M, Reuser AJ, Oostra BA. Characterization of the human lysosomal alpha-glucosidase gene. *Biochem J*, **1990**, 272: 493-497.

[4] Hoefsloot LH, Willemsen R, Kroos MA, Hoogeveen-Westerveld M, Hermans MM, Van der Ploeg AT, Oostra BA, Reuser AJ. Expression and routeing of human lysosomal alpha-glucosidase in transiently transfected mammalian cells. *Biochem J*, **1990**, 272, 485-492.

[5] Mancini GM, Beerens CE, Verheijen FW. Glucose transport in lysosomal membrane vesicles. Kinetic demonstration of a carrier for neutral hexoses. *J Biol Chem*, **1990**, 265(21),12380-12387

[6] Raben N, Takikita S, Pittis MG, Bembi B, Marie SK, Roberts A, Page L, Kishnani PS, Schoser BG, Chien YH, Ralston E, Nagaraju K, Plotz PH. Deconstructing Pompe disease by analyzing single muscle fibers: to see a world in a grain of sand. *Autophagy*, **2007**, 3(6), 546-52

[7] Nascimbeni AC, Fanin M, Tasca E, Angelini C. Molecular pathology and enzyme processing in various phenotypes of acid maltase deficiency. Neurology, 2008, 70(8), 617-26

[8] Cardone M, Porto C, Tarallo A, Vicinanza M, Rossi B, Polishchuk E, Donaudy F, Andria G, De Matteis MA, Parenti G. Abnormal mannose-6-phosphate receptor trafficking impairs recombinant alpha-glucosidase uptake in Pompe disease fibroblasts. Pathogenetics, 2008, 1(1), 6

[9] van den Hout HM, Hop W, van Diggelen OP, Smeitink JA, Smit GP, Poll-The BT, Bakker HD, Loonen MC, de Klerk JB, Reuser AJ, van der Ploeg AT. The natural course of infantile Pompe's disease: 20 original cases compared with 133 cases from the literature. Pediatrics, 2003, 112(2), 332-340

[10] Kishnani PS, Hwu WL, Mandel H, Nicolino M, Yong F, Corzo D; Infantile-Onset Pompe Disease Natural History Study Group. A retrospective, multinational, multicenter study on the natural history of infantile-onset Pompe disease. J Pediatr, 2006,148(5), 671-676

[11] Hagemans ML, Winkel LP, Van Doorn PA, Hop WJ, Loonen MC, Reuser AJ, Van der Ploeg AT. Clinical manifestation and natural course of late-onset Pompe's disease in 54 Dutch patients. Brain, 2005, 128, 671-677

[12] Van den Hout JM, Kamphoven JH, Winkel LP, Arts WF, De Klerk JB, Loonen MC, Vulto AG, Cromme-Dijkhuis A, Weisglas-Kuperus N, Hop W, Van Hirtum H, Van Diggelen OP, Boer M, Kroos MA, Van Doorn PA, Van der Voort E, Sibbles B, Van Corven EJ, Brakenhoff JP, Van Hove J, Smeitink JA, de Jong G, Reuser AJ, Van der Ploeg AT. Long-term intravenous treatment of Pompe disease with recombinant human alpha-glucosidase from milk. Pediatrics, 2004, 113(5), e448-457

[13] Klinge L, Straub V, Neudorf U, Schaper J, Bosbach T, Görlinger K, Wallot M, Richards S, Voit T. Safety and efficacy of recombinant acid alpha-glucosidase (rhGAA) in patients with classical infantile Pompe disease: results of a phase II clinical trial. Neuromuscul Disord, 2005, 15(1), 24-31

[14] Levine JC, Kishnani PS, Chen YT, Herlong JR, Li JS. Cardiac remodeling after enzyme replacement therapy with acid alpha-glucosidase for infants with Pompe disease. Pediatr Cardiol, 2008, 29(6), 1033-1042

[15] Rossi M, Parenti G, Della Casa R, Romano A, Mansi G, Agovino T, Rosapepe F, Vosa C, Del Giudice E, Andria G. Long-term enzyme replacement therapy for pompe disease with recombinant human alpha-glucosidase derived from chinese hamster ovary cells. J Child Neurol, 2007, 22(5), 565-573

[16] Kishnani PS, Corzo D, Nicolino M, Byrne B, Mandel H, Hwu WL, Leslie N, Levine J, Spencer C, McDonald M, Li J, Dumontier J, Halberthal M, Chien YH, Hopkin R, Vijayaraghavan S, Gruskin D, Bartholomew D, van der Ploeg A, Clancy JP, Parini R, Morin G, Beck M, De la Gastine GS, Jokic M, Thurberg B, Richards S, Bali D, Davison M, Worden MA, Chen YT, Wraith JE. Recombinant human acid [alpha]-glucosidase: major clinical benefits in infantile-onset Pompe disease. Neurology, 2007, 68(2), 99-109

[17] van den Hout HM, Hop W, van Diggelen OP, Smeitink JA, Smit GP, Poll-The BT, Bakker HD, Loonen MC, de Klerk JB, Reuser AJ, van der Ploeg AT. The natural course of infantile Pompe's disease: 20 original cases compared with 133 cases from the literature. Pediatrics, 2003, 112(2), 332-340

[18] Raben N, Danon M, Gilbert AL, Dwivedi S, Collins B, Thurberg BL, Mattaliano RJ, Nagaraju K, Plotz PH. Enzyme replacement therapy in the mouse model of Pompe disease. Mol Genet Metab, 2003, 80(1-2), 159-169

[19] Wenk, J, Hille, A and von Figura, K. Quantitation of Mr 46000 and Mr 300000 mannose 6-phosphate receptors in human cells and tissues. Biochem Int, 1991, 23: 723–731.

[20] Ballabio A, Gieselmann V. Lysosomal disorders: from storage to cellular damage. Biochim Biophys Acta, 2009, 1793(4), 684-696

[21] Klionsky DJ. Autophagy: from phenomenology to molecular understanding in less than a decade. Nat. Rev. Mol. Cell Biol, 2007, 8, 931-937

[22] Fukuda T, Ahearn M, Roberts A, Mattaliano RJ, Zaal K, Ralston E, Plotz PH, Raben N. Autophagy and mistargeting of therapeutic enzyme in skeletal muscle in Pompe disease. Mol Ther, 2006, 14(6), 831-9

[23] Fukuda T, Ewan L, Bauer M, Mattaliano RJ, Zaal K, Ralston E, Plotz PH, Raben N. Dysfunction of endocytic and autophagic pathways in a lysosomal storage disease. Ann Neurol, 2006,5 9(4), 700-708

[24] Roberts DJ, Tan-Sah VP, Ding EY, Smith JM, Miyamoto S. Hexokinase-II positively regulates glucose starvation-induced autophagy through TORC1 inhibition. Mol Cell. 2014;53:521–533.

[25] da-Silva WS, Gomez-Puyou A, de Gomez-Puyou MT, Moreno-Sanchez R, De Felice FG, de Meis L, et al. Mitochondrial bound hexokinase activity as a preventive antioxidant defense: steady-state ADP formation as a regulatory mechanism of membrane potential and reactive oxygen species generation in mitochondria. J Biol Chem. 2004;279:39846–39855.

# Chapter 1.

## Acid-alpha glucosidase interactions and pathophysiology of Pompe Disease.

## INTRODUCTION AND OBJECTIVES

It is now clear that in PD, as well as in the others lysosomal storage diseases (LSDs), substrate storage leads to several alterations in cellular functions and pathways. Multiple abnormalities of cell morphology, including lysosomal and cytoplasmic glycogen accumulation, the presence of multivesicular bodies, the disruption of the normal structure of the Golgi apparatus, were observed in fibroblasts cultured from PD patients with the different clinical forms of the disease both by electron microscopy analysis and by immunofluorescence studies [1]. The abnormalities of the Golgi apparatus were associated with changes in the distribution of CI-MPR, a membrane-bound protein mostly localized in these organelles. CI-MPR traffics within cells following different itineraries, such as the lysosomal enzyme biosynthetic pathway and the endosomal pathway; along these routes transit through the trans-Golgi network is an important stage. The finding of increased co-localization of the CI-MPR with LC3, a marker of the autophagosomes and autophagolysosomes, supported the hypothesis of an impaired retrograde trafficking of the receptor from late endosomes to the trans-Golgi network, and indicated that, at least in part, CI-MPR is sequestered in relatively inert vesicles deriving from the fusion of autophagosomes with substrate-engulfed lysosomes. An important consequence of the sequestration of CI-MPR in these organelles, is a depletion of functionally available CI-MPR at the plasma membrane. It is becoming clear that secondary cellular abnormalities may negatively affect the efficacy of the therapies currently available, thus providing clues to clarify the reasons for the variable response of different patients and tissues to therapies. Correction of secondary cellular abnormalities may represent an additional and novel target of therapy.

Moreover, impaired intracellular trafficking of vesicles and altered membranes and membrane-bound proteins have been described but there are no evidence about the

mechanisms underlying these events. Aberrant membrane cholesterol and SNARE levels in LSDs cells may determine lysosomal and endocytic traffic dysfunctions [2], but also some aberrant protein interactions could constitute additional factors that contribute to the occurrence of abnormalities of vesicle trafficking and CI-MPR distribution in PD. In view of these considerations, we have analyzed protein interactions in PD.

This project has been focused on the investigation of the intracellular pathways controlling GAA trafficking and how they change in the presence of amino acid mutations impairing GAA activity in order to understand the role of these interactions in PD pathophysiology.

## RESULTS

Preliminary data obtained in collaboration with the Department of Chemical Sciences and CEINGE suggested that wild type GAA has several protein interactors (***Table 1***). In particular, Immunoprecipitation (IP) experiments and analysis of Nanoliquid Chromatography-Tandem Mass Spectrometry (nanoLC-MS/MS) on protein extracts from control fibroblasts showed a list of wild type GAA protein interactors and, surprisingly, most of them belong to the cytoskeleton. Recently, it has been shown that some cytoskeleton-associated proteins (i.e. myosin 1G (MYO1G), myosin heavy chain 1 (MYH1) and tropomyosin 2 (TPM2) ) are essential for lysosomal stability in human breast cancer cells and their inactivation by the use of specific siRNAs induced several changes in the endo-lysosomal compartment, such as an increased lysosomal volume, an altered lysosomal localization, and a reduced autophagic flux [3]. Therefore this results seems to be very interesting. So, we selected some of these proteins to confirm the preliminary results obtained with nanoLC-MS/MS.

| GAA Protein Interactors by nano LC-MS/MS | |
|---|---|
| **BAND** | **PROTEIN** |
| **2** | **Plectin** (Hemidesmosomal protein 1; PLEC) |
| **7** | **Unconventional myosin-VI** (MYO6) |
| **8** | **Unconventional myosin-Ic** (Myosin I beta; MYO1C) |
| **9** | **Unconventional myosin-Ib** (MYH-1c; MYO1B) |
| **11** | **Lysosomal alpha-glucosidase** (GAA) |
| **12** | **Gelsolin** (Actin-depolymerizing factor; GSN) |
| | **Unconventional myosin-Id** (MYO1D) |
| **18** | **Coronin-1C** (Coronin-3; CORO1C) |
| **23** | **Tropomodulin-3** (TMOD3) |
| **27** | **Tropomyosin alpha-1 chain** (Tropomyosin-1; TPM1) |
| **30** | **Tropomyosin alpha-4 chain** (Tropomyosin-4; TPM4) |
| | **Tropomyosin 3** (Tropomyosin alpha-3 chain; TPM3) |
| **31** | **Tropomyosin beta chain** (Tropomyosin-2; TPM2) |
| **37** | **Lysosomal alpha-glucosidase** (GAA) |
| | **60S ribosomal protein L12** (RPL12) |

**Table. 1** This table describe possible wild type GAA protein interactors obtained by Immunoprecipitation (IP) experiments and nanoLC-MS/MS analysis on protein extract from control fibroblasts. This data have been obtained in collaboration with the Department of Chemical Sciences and CEINGE.

We have further confirmed these interactions by immunoprecipitation studies and western blot analysis.

*Myosin 1C*

Class 1 myosins are particularly interesting, since they can simultaneously associate with membranes and actin filaments [4], thereby regulating membrane– cytoskeleton adhesion [5]. Accordingly, they participate in endocytosis, exocytosis, and regulation of tension between the cytoskeleton and the plasma membrane [6].

It has been shown that a myosin I family member (MYO1C) is required for optimal insulin-stimulated translocation of intracellular membranes containing GLUT4 glucose transporters to the plasma membrane [7]. In light of this finding, and of the fact that MYO1C is one of the GAA interacting protein found by nanoLC-MS/MS analysis, we

decided to validate the interaction between MYO1C and GAA by co-immunoprecipitation and western blot analysis.

Total extract from control fibroblasts were incubated with magnetic beads linked to anti GAA antibody that retains GAA and other proteins interacting with GAA. Complexes were eluted from beads and analyzed by western blot analysis revealing for MYO1C (***Fig. 2***).

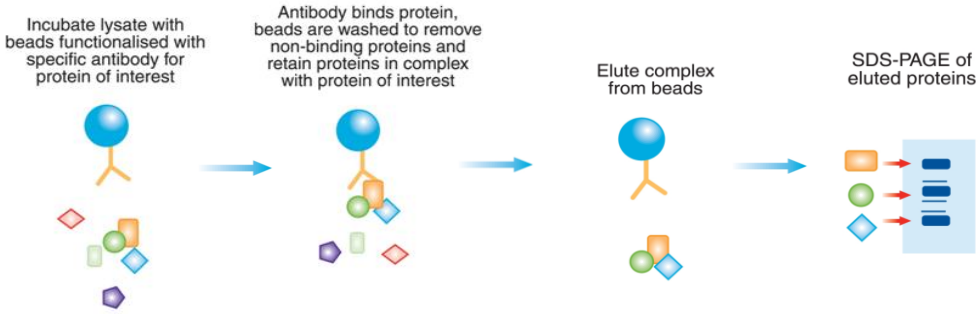


**Fig. 2** Picture representing the co-immunoprecipitation analysis steps.

Total extract were also immunoprecipitated with Myo 1C antibody and revealed for GAA by western blotting. As negative control, total extracts were incubated in absence of antibodies. The interaction between these two proteins was confirmed in both the experiments (***Fig. 3***).

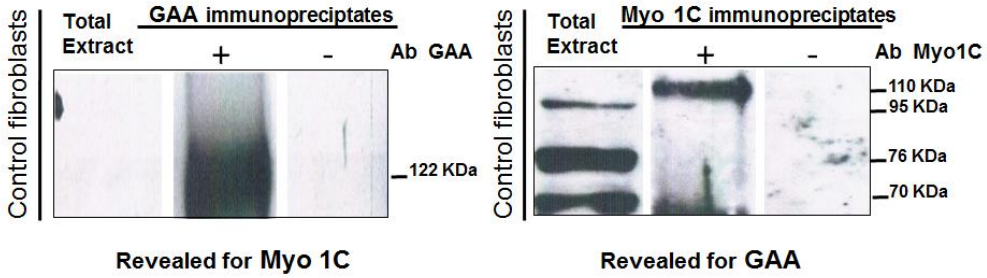


**Fig. 3** Western blot analysis of GAA-MYO1Cco-immunoprecipitations. The left panel shows the detection of MYO1C on GAA immunoprecipitates obtained from control fibroblasts. The right panel shows the detection of GAA in MYO1C immunoprecipitates. The negative controls (third lanes) represents the cell lysates incubated without antibody. The results confirm the interaction between the two proteins.

*Tropomyosin 3*

Tropomyosin was primarily regarded as a muscle protein that regulates the interaction of actin-containing thin filaments with myosin filaments to allow contraction [8]. Multiple tropomyosin isoforms are also expressed in non-muscle cells where tropomyosins participate in a number of cytoskeleton-mediated cellular processes [9, 10]. A widely accepted function of tropomyosins in non-muscle cells is to stabilize actin filaments mechanically, and possibly to protect against the action of filament-destabilizing proteins and disassembling drugs [11].

To validate the interaction between GAA and tropomyosin 3 (TPM3) we performed co-immunoprecipitation and western blot analysis on total extract from control fibroblasts in the same conditions used for GAA-MYO1C co-immunoprecipitation analysis (***Fig. 4***). The results of these experiments confirm the interaction between GAA and TPM3.

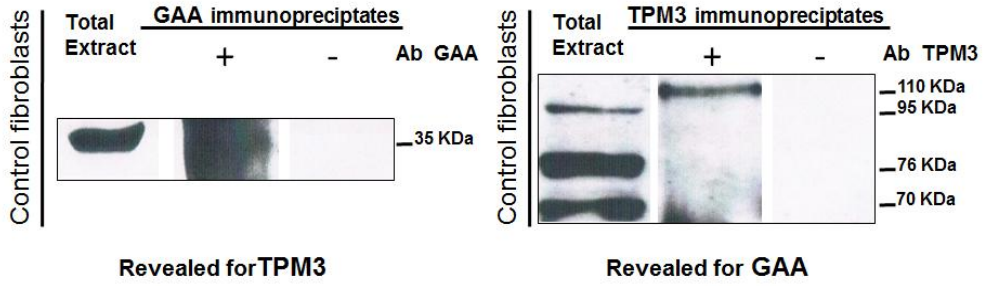


**Fig. 4** Western blot analysis of GAA-TPM 3 co-immunoprecipitations. The first panel shows the detection of TPM3 on GAA immunoprecipitates from control fibroblasts, the opposite in the second panel. Also in this case the interaction between GAA and TPM3 was confirmed.

*Myosin VI*

Myosin VI (MYO6) is a 140 kDa ATP-sensitive actin binding protein that consists of an N-terminal highly conserved motor domain that can bind ATP and filamentous actin (***Fig. 5***). It is followed by a neck region and a C-terminal tail domain. Between the motor domain and neck region there is an addictional unique 53 amino acid insert which has been predicted to be the “reverse gear” that allows MYO6 to move towards the minus end of actin filaments [12]. Unexpectedly this insert has recently been shown to bind calmodulin [13] despite not containing a recognizable IQ-calmodulin binding motif.

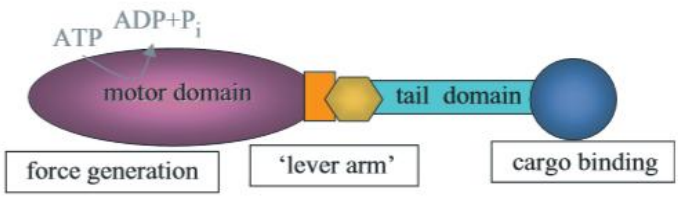


**Fig. 5** Myosin VI is an ATP-sensitive actin binding protein that consists of an N-terminal highly conserved motor domain that can bind ATP and filamentous actin. It is followed by a neck region and a C-terminal tail domain.

Myosin of class VI has the unique ability, unlike the rest of the myosin family, to translocate towards the pointed or minus end of actin filaments [14]. In mammalian cells, MYO6 has been shown to be involved in endocytosis, in membrane ruffling at the

leading edge of cells and in the maintenance of Golgi complex morphology and in secretion. Cellular localization studies have confirmed that MYO6 is present in clathrin-coated and uncoated vesicles distributed throughout the cell, in membrane ruffles and in the Golgi complex network [15]. MYO6 involvement in endocytosis and in maintenance of Golgi morphology (both affected in PD cells morphology) and its possible interaction with wild type GAA suggest that this protein could have a role in GAA trafficking from ER to lysosome.

To further investigate the interactions between GAA and MYO6, we also performed co-immunoprecipitation studies on protein extract from control and mutant fibroblasts (***Fig. 6***). We decided to select fibroblasts from a patient homozygous for the p.L552P GAA gene mutation. This mutation is associated with the synthesis of a misfolded protein and with a residual enzyme activity. MYO6 seems to interact with both wt and mutant GAA; in particular, in MYO6 immunoprecipitates different isoforms of the enzyme are represented (a 95 kDA precursor isoform and the two 76 and 70 kDa mature forms).

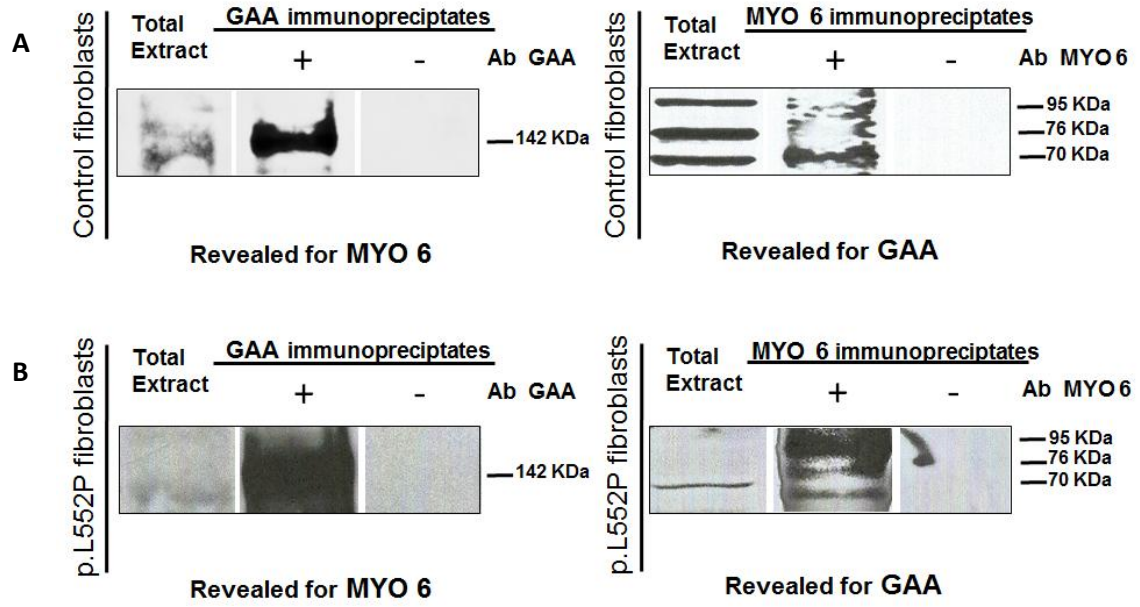


**Fig.6** Western blot analysis of GAA-MYO6 co-immunoprecipitations. **A**) The first panel shows the detection of MYO6 on GAA immunoprecipitates obtained from control fibroblasts.The second one shows the detection of GAA on MYO6 immunoprecipitates.The results confirm the interaction between GAA and MYO6.**B**) The first panel shows the detection of MYO6 on GAA immunoprecipitates from L552P fibroblasts, the opposite in the second panel. Also in this case the interaction between GAA and MYO6 was confirmed. MYO6 shows interaction with both wt and mutant GAA.

*Gelsolin*

Gelsolin (GSN) is the most potent actin filament severing protein identified to date. Severing is the weakening of enough non-covalent bonds between actin molecules within a filament to break the filamentin two [16]. GSN is composed of six domains, designated (from the N-terminus) as G1–G6 (***Fig. 7***). Each domain contains $Ca^{2+}$-binding site. The helical tail is in close contact with the actin binding helix of G2 and may act as a latch to inhibit actin binding. Recent studies show that residues in the $Ca^{2+}$-binding sites of G2 and G6 are involved in regulating GSN structure, including stabilizing the $Ca^{2+}$-free state, promoting transitions through intermediate states and stabilizing the $Ca^{2+}$-bound state. $Ca^{2+}$-binding by G2 is critical in the activation and stabilization of GSN [17]. The disulfide bond in G2 is involved in $Ca^{2+}$ activation of GSN. The most extensively examined roles of GSN relate to its ability to sever, cap, uncap,

and nucleate actin filaments. GSN can bind to actin monomers and filaments, and is regulated by pH, phosphoinositides, lysophosphatidic acid, and high micromolarconcentrations of $Ca^{2+}$ [18]. The GSN capability to interact with actin and to regulate its polymerization, associated with its possible interaction with GAA, led us to focus on this protein. In fact, studies in GAA knock-out mice showed that the presence of glycogen-filled lysosomes in muscle fibers interferes with the architecture and function of the contractile apparatus with a mechanical effect [19]. X-ray diffraction studies showed that, although the content of contractile proteins was equivalent, actin and myosin filaments were disordered in the PD muscle, and that actin and myosin interactions were disrupted. Moreover, in 2009 Kelly et al showed that GSN alteration is involved in Familial amyloidosis of Finnish type (FAF) or gelsolin amyloidosis. The D187N/Y mutation in plasma GSN enables an aberrant protein cleavage, generating a 68-kDa fragment (C68) of GSN that is secreted. C68 can be further cleaved in the extracellular space to generate amyloidogenic fragments. Deposition occurs in skeletal and cardiac muscle, leading to cardiomyopathy and muscle weakness [20], that are also the clinical manifestations of PD. Furthermore, it has been shown that gelsolin can bind lipids and can become partially embedded in vesicle membranes at low pH values within the physiologically normal range [21] and that it can also control transport of the autonomous parvovirus Minute Virus of Mice from the nucleus to the cell periphery and release into the culture medium by (virus-modified)lysosomal/late endosomal vesicle transport [22]. All together these evidences led us to further investigate about the possible interaction between GSN and GAA and its functional role.

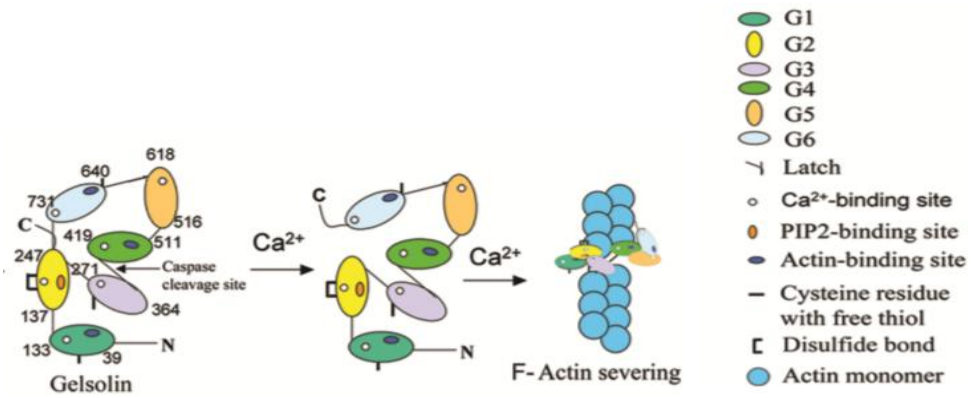


**Fig. 7** Gelsolin has three different actin binding domains which are distributed within the six repeating segments (G1–G6) in the amino acid sequence of gelsolin. Monomer actin binding sites are present in segment G1 and G4–6, while the highest affinity F-actin binding site is located in G2–3.

GSN exists in extracellular (secreted, pGSN) and intracellular (cytoplasmic, cGSN) forms, both of which are encoded by a single gene on chromosome 9 [23] in humans and on chromosome 2 in mouse, and are under the control of different promoters. The gene that codes both GSN isoforms is made up of at least 14 distinct exons which span a region of 70 kb. The arrangement of cGSN at the 5'-end is exon 1-intron-exon 2-intron-exon 4. Collectively, exons 1 and 2, which are 13 kb apart in the gene, make up the unique 5' untranslated region of cGSN. The 5'-end of the pGSN differs from the cGSN, as it is made up of exon3-intron-exon 4. Exon 3, which is found 2.3 kb upstream from exon 4, comprises a small region of untranslated sequence and codes for both the signal peptide and the first 21 residues of the pGSN [24] (***Fig. 8***).

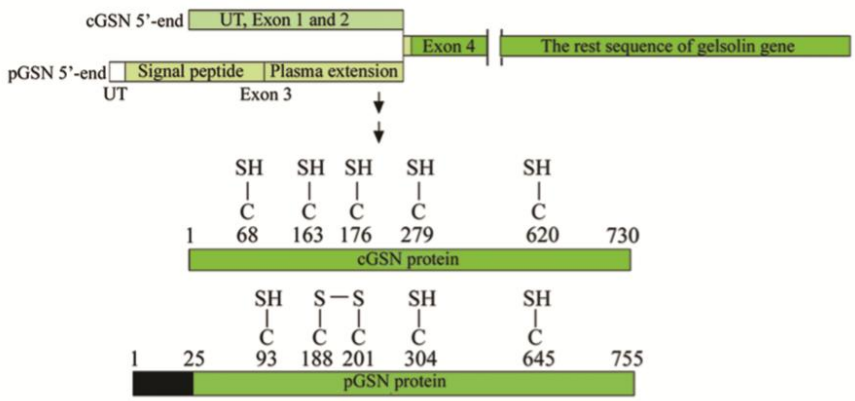


**Fig. 8**The human gene that codes both GSN isoforms is made up of at least 14 distinct exons which span a region of 70kb. The arrangement of cGSN at the 5'-end is exon 1-intron-exon 2-intron-exon 4. The 5'-end of the pGSN differs from the cGSN, as it is made up of exon3-intron-exon 4.

Secreted GSN differs from intracellular gelsolin in having a signal peptide, a 25-residue amino-terminal extension and a disulphide bond between cysteines 188 and 201. Plasma GSN is larger than cytoplasmic GSN (Mr 93,000 versus 90,000, respectively) and is more positively charged. The two GSN share a common 29 amino acid sequence which lies at the NH-terminal end of cytoplasmic GSN and spans residues 26-55 of plasma GSN. Compared with cytoplasmic GSN, plasma GSN contains an additional peptide of 25 amino acids at its NH terminus.These two forms are structurally similar but not identical and after synthesis these proteins are processed independently, and have a distinct fate [24].

My study has been especially focused on the interaction between GAA and GSN. Western blot analysis of GAA-GSN co-immunoprecipitations showed that, unlike MYO6, GSN interacts with wild type GAA but there is no interaction with mutant GAA. Moreover, GSN appeared to interact mainly with the precursor (95 KDa) GAA isoform (***Fig.9***).

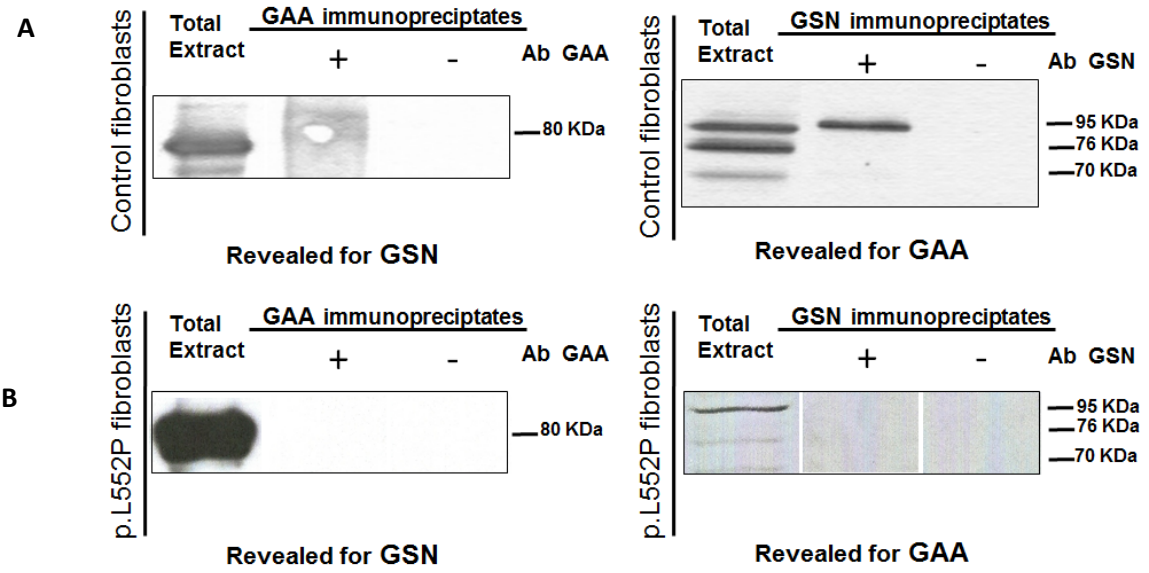


**Fig. 9** Western blot analysis of GAA-GSN co-immunoprecipitations. **A**) The first panel shows the detection of GSN on GAA immunoprecipitates obtained from control fibroblasts.The second one shows the detection of GAA on GSN immunoprecipitates.The result confirm the interaction between GAA and GSN.**B**) The first panel shows the detection of GSN on GAA immunoprecipitates from L552P fibroblasts, the opposite in the second panel. GSN interacts with wild type GAA but there is no interaction with mutant GAA. Moreover, GSN appears to interact mainly with the precursor (95 KDa) GAA isoform.

The interaction between GAA and GSN was not evident by immunofluorescence confocal microscopy experiment on control fibroblasts, because of the diffuse cytoplasmic distributionof GSN signal pattern.To circumvent this problem we performed a Proximity Ligation Assay (PLA) in control fibroblasts. This immunoassay employes species-specific secondary antibodies, called PLA probes, each with a unique short DNA strand attached to it. When the PLA probes are in close proximity (in case of protein interaction), the DNA strands can interact through a subsequent addition of two other circle-forming DNA oligonucleotides. After joining of the two added oligonucleotides by enzymatic ligation, they are amplified via rolling circle amplification using a polymerase, in presence of nucleotides and fluorescently labeled oligonucleotides. The resulting high concentration of fluorescence in each single-molecule amplification product is easily visible as a distinct bright spot when viewed with a fluorescence microscope (***Fig.10***). As positive control we used the interaction

between Actin and GSN, in which we observed several red dots; as negative control we used GSN-LAMP2 staining that is associated with the absence of red dots. In GAA-GSN staining we observed red dots in small but detectable amount and this result seems to confirm the interaction between GAA and GSN in control fibroblasts.

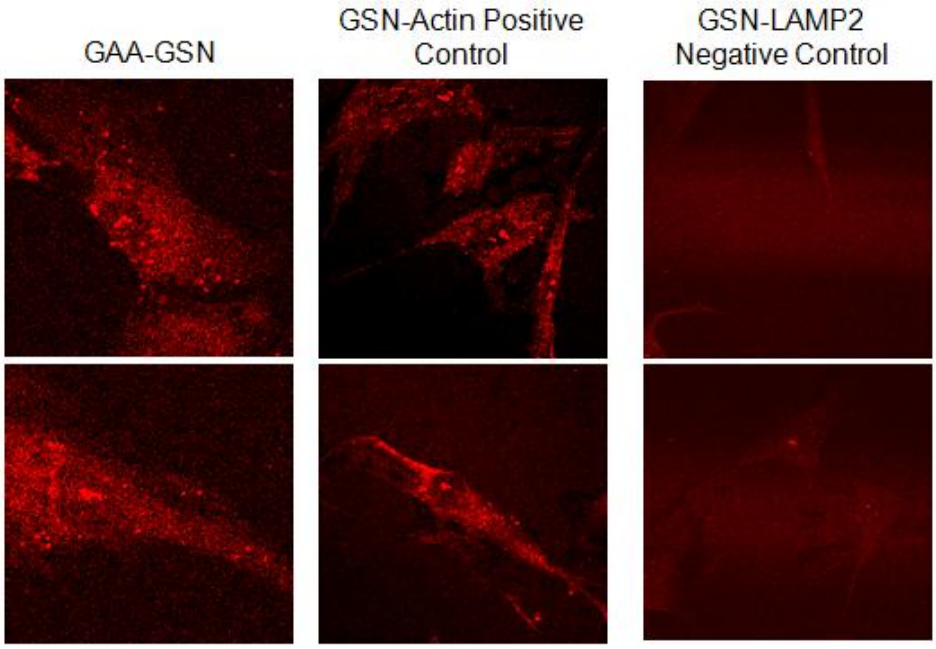


**Fig. 10** Proximity Ligation Assay on control fibroblasts. GSN-Actin staining is the positive control, GSN-LAMP2 the negative control. The results seem to confirm the interaction between GAA and GSN in control fibroblasts.

Confocal microscopy immunofluorescence experiments in L552P fibroblasts showed that GSN signal seems to be more represented in L552P fibroblasts than in control fibroblasts (***Fig. 11***). We also performed western blot analysis in three control fibroblast and five PD fibroblast lines, obtained from patients with different phenotypes among them. In all patients there is a significant increase in the amount of GSN and the appearance of a 68 kDa GSN band. We have supposed that this band can be a cleavage product in PD fibroblasts but this suggestion have to be confirmed.

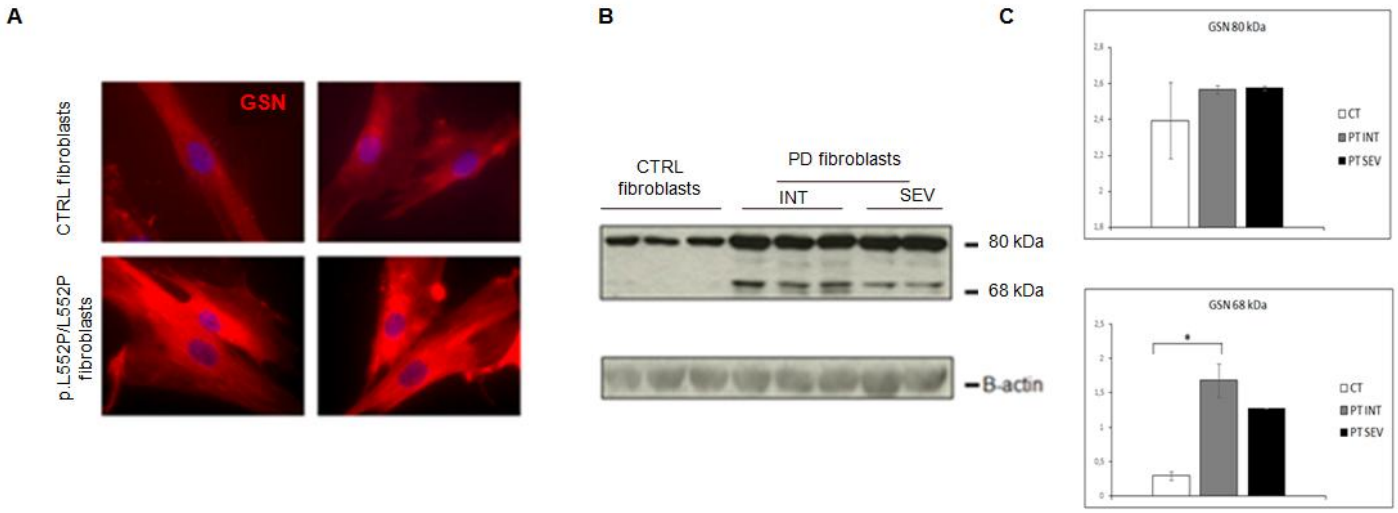


**Fig. 11 A)** Confocal microscopy analysis of Gelsolin distribution. The GSN signal seems to be more represented in L552P fibroblasts. **B)** Western Blot analysis of GSN isoforms. Quantitative analysis of the bands by ImageJ (right). Five PD fibroblast cell lines show a 68 kDa band in addition to the typical 80 kDa band. **C)** Quantitaive analysis of GSN isoforms.* *p< 0,01*

Moreover, we have performed some analysis in a group of BALB/c GSN KO mice, in collaboration with Ronchi's group at Bicocca University in Milan. Primary fibroblasts from WT and GSN KO mice were obtained from peritoneal biopsy. In order to evaluate the possible effect of GSN absence on GAA trafficking and maturation, we performed western blot analysis on fibroblasts lysates from WT and GSN KO mice. We used human control fibroblasts as positive control and PD human fibroblasts as negative control (Figure 12). Results showed the presenceof the mature and active form of GAA both in WT and GSN KO mice, but the pattern of the different isoforms of the enzyme seems to be different between GSN WT and KO. The reason of this result is not clear and further studies are necessary to clarify this point.

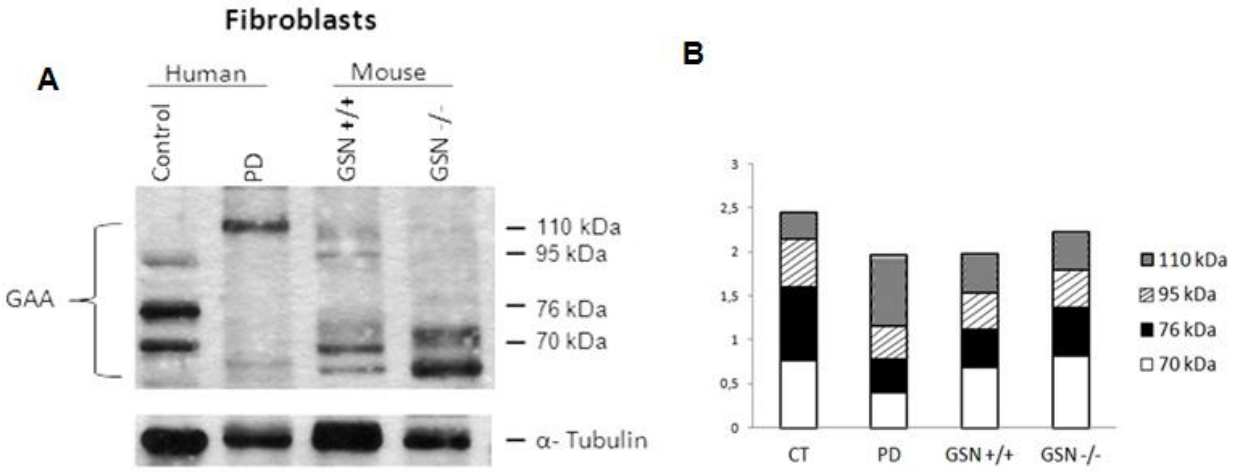


**Fig. 12 A)** Western blot analysis on fibroblasts lysates from WT and GSN KO mice. Control fibroblasts were used as positive control and PD human fibroblasts as negative control. **B)** Quantitative analysis of the different enzyme isoforms.

## METHODS

*Cell Culture*

Fibroblasts from control individuals and from PD patients were obtained from the cell repository at the Department of Traslational Medicine, Università degli Studi di Napoli Federico II.Fibroblasts were grown in DMEM medium supplemented with fetal bovine serum, L-glutamine and antibiotics.

*Immunoprecipitation and Western Blot*

Fibroblasts protein extracts were obtained by lysing cells with 2,5mM KCl, 150mM NaCl, 50 mM Tris HCl pH 6.5, 0.1% Triton X-100 and protease inhibitors for 30 minutes at 4°C. samples were centrifuged at 13000 rpm fot 30 minutes at 4°C. The supernatant constituted the protein extract. 1 milligrams of protein extract were immunoprecipitated with 20 µl of Dynabeads protein G (Life technologies AS, Oslo) and 4 µl of antibody to GAA (rabbit polyclonal antibody provided by PRIMM) and 4 µg of antibody to GSN (Abcam) and MYO6 (LSBio) over night. Immunoprecipitated were immunoblotted and visualized with the chemiluminescent substrate ECL (GE Healthcare, Milan, Italy).

*Confocal microscopy analysis*

For immunofluorescence (IF), fibroblasts were seeded on chamber slides, fixed with 4% paraformaldehyde (PFA), treated with 0.1% Triton, incubated in blocking solution (0.5% BSA, 10% horse serum in PBS) for 20min, and then incubated overnight at 4°C with antibodies (the same used for immunoprecipitation, see above). Appropriate secondary fluorescent antibodies (Alexa-Fluor, Invitrogen,Paisley, UK) were used. Slides were mounted using Vectashild medium with DAPI stain (Vector, Burlingame, CA, USA) and

examined on a fluorescence Leica DM5000B microscope (Leica Microsystems Srl, Milan, Italy).

*GAA activity assay*

GAA activity was assayed by using the fluorogenic substrate 4-methylumbelliferyl-α-D-glucopyranoside (Sigma-Aldrich). Briefly, 25 µg of protein were incubated with the fluorogenic substrate (2mmol/l) in 0,2 mol/l acetate buffer, pH 4.0, for 60 minutes in incubation mixtures of 20 µl. The reaction was stopped by adding 1 ml of glycine-carbonate buffer, pH 10.7. Fluorescence was read at 365 nm (excitation) and 450 nm (emission) on a Turner Biosystem Modulus fluorometer.

*Proximity Ligation Assay (PLA)*

For PLA (OLINK Bioscience), fibroblasts were seeded on chamber slides, fixed and permeabilized with Methanol for 10 min at -20°C and Acetone for 1 min at -20°C, incubated in blocking solution (1% BSA in PBS) for 15 min, and then incubated for 2 hours with primary antibodies (the same used for immunoprecipitation, see above). Appropriate secondary antibodies were used. Fixed cells were incubated with PLA Probe for 1 hour at 37°C. Enzymatic ligation of the probes was performed by adding the ligation solution for 30 min at 37°C. Finally, the amplification solution was added and cells were incubated for 1 hour and 40 min at 37°C. Slides were mounted using Vectashild medium with DAPI stain (Vector, Burlingame, CA, USA) and examined on a fluorescence Leica DM5000B microscope (Leica Microsystems Srl, Milan, Italy).

## CONCLUSIONS

PD is a metabolic myopathy caused by the deficiency of the lysosomal hydrolase GAA. Secondary abnormalities, such as altered Golgi and trans-Golgi network morphology and abnormal distribution of CI-MPR, play a major role in the occurrence of cell damage and muscular atrophy. The presence of these abnormalities led us to also investigate about the protein interacting with the GAA. Immunoprecipitation (IP) experiments and analysis of nanoLC-MS/MS on protein extract from human control fibroblasts showed a list of wild type GAA protein interactors and most of them belong to the cytoskeleton. In particular, we focused on some of this interactions. Co-immunoprecipitations and western blot analysis confirmed the GAA interaction with MYO1C, TPM3 and MYO6. In particular, we observed that MYO6 interact with both wt and mutant GAA.

We focused on Gelsolin, a cytoskeleton protein that, when altered, is responsible of a Familial amyloidosis (FAF) that presents some clinical manifestations similar to PD, such as cardiomyopathy and muscle weakness [50]. Furthermore, there are evidences about its involvement in vescicle membrane structure at specific pH conditions [52]. Western blot analysis of GAA-GSN co-immunoprecipitations showed that, unlike MYO6, GSN interacts with wild type GAA but there is no interaction with mutant GAA. Moreover, GSN appeared to interact mainly with the precursor (95 KDa) GAA isoform. This result suggested us that gelsolin can probably have a role in the first steps of GAA trafficking from ER to lysosome, where it is processed to the mature isoform, but so far its function is not clear. In order to confirm this interaction, we performed a Proximity Ligation Assay (PLA) in human control fibroblasts that revealed positive signals of GAA-GSN interaction.

GSN staining in human control and PD fibroblasts showed that GSN seems to be more abundant in mutant cells, in which there is the misfolded enzyme that is no properly

processed to lysosomes. These data were confirmed also by western blot analysis in PD and control fibroblasts. The same analysis showed the appearance of a 68 kDa GSN band in PD fibroblast, that seemed more abundant in intermediate patients, compared to severe. This band reminds to the 68 kDa cleaved fragment in FAF, so we have supposed that the 68 kDa band could be a cleavage product in PD cells. Obviously, this hypothesis needs to be further validated.

The suggestion of a possible role of GSN in GAA maturation, has been supported by western blot analysis in fibroblasts from WT and GSN KO mice. Results showed the presence of the mature and active form of GAA both in WT and GSN KO mice, but the pattern of the different isoforms of the enzyme seemed to be different between GSN WT and KO. The reason of this result is not clear and further studies are necessary to clarify this point.

All together this results lead us to further investigate about this novel interaction, whose meaning is still unclear. It is well known that in PD, such as in all LSD, there are impaired intracellular trafficking, abnormal distribution of CI-MPR and aberrant Golgi and trans-Golgi network morphology, but the molecular mechanisms underlying these events are still unknown. Our ongoing objectives is to further investigate about this interactions and to identify proteins and pathways involved in PD cellular abnormalities in order to improve our understanding of PD pathophysiology and to characterize new therapeutic targets.

## BIBLIOGRAPHY


[1] Cardone M, Porto C, Tarallo A, Vicinanza M, Rossi B, Polishchuk E, Donaudy F, Andria G, De Matteis MA, Parenti G. Abnormal mannose-6-phosphate receptor trafficking impairs recombinant alpha-glucosidase uptake in Pompe disease fibroblasts. *Pathogenetics*, **2008**, 1(1), 6

[2] Fraldi A1, Annunziata F, Lombardi A, Kaiser HJ, Medina DL, Spampanato C, Fedele AO, Polishchuk R, Sorrentino NC, Simons K, Ballabio A. Lysosomal fusion and SNARE function are impaired by cholesterol accumulation in lysosomal storage disorders. *EMBO* J. 2010 Nov 3;29(21):3607-20.

[3] Groth-Pedersen L1, Aits S, Corcelle-Termeau E, Petersen NH, Nylandsted J, Jäättelä M.Identification of cytoskeleton-associated proteins essential for lysosomal stability and survival of human cancer cells.PLoS One. Epub 2012 Oct 11.

[4] McKenna JM, Ostap EM. Kinetics of the interaction of myo1c with phosphoinositides. J Biol Chem. 2009 Oct 16;284(42):28650-9. doi: 10.1074/jbc.M109.049791. Epub 2009 Aug 25.

[5] Nambiar R1, McConnell RE, Tyska MJ. Control of cell membrane tension by myosin-I. Proc Natl Acad Sci U S A. 2009 Jul 21;106(29):11972-7.

[6] McConnell RE1, Tyska MJ. Leveraging the membrane - cytoskeleton interface with myosin-1. Trends Cell Biol. 2010 Jul;20(7):418-26.

[7] Bose, A., A. Guilherme, S. I. Robida, S. M. C. Nicoloro, Q. L. Zhou, Z. Y. Jiang, D. P. Pomerleau, and M. P. Czech. Glucose transporter recycling in response to insulin is facilitated by myosin Myo1c. 2002. Nature 420:821– 824

[8] Perry SV Vertebrate tropomyosin: distribution, properties and function. J Muscle Res Cell Motil 22,5–49, 2001

[9] Gunning P, O'Neill G & Hardeman E. Tropomyosin-based regulation of the actin cytoskeleton in time and space. Physiol Rev 88,1 –35, 2008.

[10] Dominguez R. Tropomyosin. The gatekeeper's view of the actin filament revealed. Biophys J 100, 797–798, 2011.

[11] Cooper JA. Actin dynamics: tropomyosin provides stability. Curr Biol 12, R523–R525, 2002.

[12] Wells AL1, Lin AW, Chen LQ, Safer D, Cain SM, Hasson T, Carragher BO, Milligan RA, Sweeney HL. Myosin VI is an actin-based motor that moves backwards. Nature. 1999 Sep 30;401(6752):505-8.

[13] Bahloul A1, Chevreux G, Wells AL, Martin D, Nolt J, Yang Z, Chen LQ, Potier N, Van Dorsselaer A, Rosenfeld S, Houdusse A, Sweeney HL. The unique insert in myosin

VI is a structural calcium-calmodulin binding site. Proc Natl Acad Sci U S A. 2004 Apr 6;101(14):4787-92. Epub 2004 Mar 22.

[14] David A. Tumbarello, John Kendrick-Jones, and Folma Buss. Myosin VI and its cargo adaptors – linking endocytosis and autophagy.

[15] Warner CL1, Stewart A, Luzio JP, Steel KP, Libby RT, Kendrick-Jones J, Buss F. Loss of myosin VI reduces secretion and the size of the Golgi in fibroblasts from Snell's waltzer mice. EMBO J. 2003 Feb 3;22(3):569-79.

[16] Mejillano, Helen L. Yin and Hui Qiao Sun, Masaya Yamamoto, Marisan. Regulatory Protein Gelsolin, a Multifunctional Actin J. Biol. Chem. 1999, 274:33179-33182

[17] Nag S, Ma Q, Wang H, Chumnarnsilpa S, Lee WL, Larsson M, Kannan B, Hernandez-Valladares M, Burtnick LD, Robinson RC. Ca21 binding by domain 2 plays a critical role in the activation and stabilization of gelsolin. Proc Natl Acad Sci USA 2009;106:13713–13718.

[18] Meerschaert K, De Corte V, De Ville Y, Vandekerckhove J, Gettemans J. Gelsolin and functionally similar actin-binding proteins are regulated by lysophosphatidic acid. EMBO J 1998;17:5923–5932.

[19] Sengen Xu, Mikhail Galperin, Gary Melvin, Robert Horowits, Nina Raben, Paul Plotz, Leepo Yu. Impaired organization and function of myofilaments in single muscle fibers from a mouse model of Pompe disease. Journal of Applied Physiology Published 1 May 2010 Vol. 108 no. 5, 1383-1388

[20] Page LJ1, Suk JY, Bazhenova L, Fleming SM, Wood M, Jiang Y, Guo LT, Mizisin AP, Kisilevsky R, Shelton GD, Balch WE, Kelly JW. Secretion of amyloidogenic gelsolin progressively compromises protein homeostasis leading to the intracellular aggregation of proteins. Proc Natl Acad Sci U S A 2009 Jul 7 ;106(27):11125-30

[21] Méré J1, Chahinian A, Maciver SK, Fattoum A, Bettache N, Benyamin Y, Roustan C. Gelsolin binds to polyphosphoinositide-free lipid vesicles and simultaneously to actin microfilaments. Biochem J. 2005 Feb 15;386(Pt 1):47-56.

[22] Bär S1, Daeffler L, Rommelaere J, Nüesch JP. Vesicular egress of non-enveloped lytic parvoviruses depends on gelsolin functioning. PLoS Pathog. 2008 Aug 15;4(8):e1000126.

[23] Yin HL, Kwiatkowski DJ, Mole JE, Cole FS. Structure and biosynthesis of cytoplasmic and secreted variants of gelsolin. J Biol Chem. 1984 Apr 25;259(8):5271-6

[24] Guo Hua Li, Pamela D. Arora, Yu Chen, Christopher A. McCulloch, and Peter Liu. Multifunctional Roles of Gelsolin in Health and Diseases. Wiley Online Library 9 November 2010

# Chapter 2

# Oxidative stress and PD

## INTRODUCTION

- **Autophagic accumulation in Pompe disease**

The recent advancements in the knowledge of lysosomal biology and function have translated into a better understanding of the pathophysiology of LSDs. It is now clear that the clinical manifestations of these disorders are not only the direct effects of storage, but derive also from a cascade of secondary events that lead to dysfunction of several cellular processes and pathways. These processes include: secondary storage of substrates unrelated to the defective enzyme; abnormal composition of membranes, and their consequences on vesicle fusion and trafficking; impairment of autophagy; alteration of signaling pathways; oxidative stress; abnormalities of calcium homeostasis; and several others. Particular attention has been paid to the derangement of autophagy. In recent years it has been shown that a failure of productive autophagy in muscle tissue contributes strongly to disease pathology in PD patients [1]. Shea and Raben found an accumulation of autophagic vesicles in Type II-rich muscle fibers in the GAA knock-out mouse model and they showed that this build-up of autophagosomes disrupts the contractile apparatus in the muscle fibers [1]. Furthermore, the recombinant enzyme, given by ERT, uses the endocytic pathway to deliver the lysosomes, so it became clear that massive accumulation of autophagic material in muscle would interfere with the recombinant enzyme in ERT [2,3]. In fact, it has been shown that in muscle fibers from wild-type mice, rhGAA is efficiently targeted to lysosomes, while in GAA knock-out muscle fibers, most of the endocytosed recombinant enzyme is accumulated in the central autophagic area and very little reached the lysosomes [1, 4].

- **Increased oxidative stress in Pompe disease**

It is reasonable to think that other pathways are dysregulated in PD and oxidative stress (ox-stress) appears to be interesting in this aspect. Increased ox-stress has been reported in different LSDs [5, 6]. In particular, Lim at al. have found multiple mitochondrial defects in mouse and human models of Pompe disease: a profound dysregulation of $Ca^{2+}$ homeostasis, mitochondrial $Ca^{2+}$ overload, an increase in reactive oxygen species, a decrease in mitochondrial membrane potential, an increase in caspase-independent apoptosis, as well as a decreased oxygen consumption and ATP production of mitochondria [7]. Moreover, they showed distended mitochondria with disarrayed cristae, often adjacent to the area of autophagic buildup, in muscle from GAA KO mice. These data are consistent with observations of changes in the morphology of mitochondria in muscle biopsies from Pompe patients. Cytosolic Ca2+ is significantly higher in KO myotubes and treatment with recombinant human GAA (rhGAA) results in a moderate decrease in $Ca^{2+}$ levels [7].

- **Autophagic pathway and oxidative stress**

Increased ox-stress is one of the potential factors implicated in induction of autophagy. Indeed, ox-stress has been recognized as an important activator of autophagy [8, 9].
Autophagy has been seen as an adaptive response to stress, which promotes survival. The regulatory pathways of autophagy acts in response to nutrients deprivation; in the extreme case of starvation, the breakdown of cellular components promotes cellular survival by maintaining cellular energy levels [9,10, 11].

The activation of autophagy in response to cellular needs is controlled by the mammalian target of rapamycin complex 1 (mTORC1) [12]. Active mTORC1 controls the activity of protein translation by direct phosphorylation of two key protein targets,

EIF4E-binding protein 1 (4E-BP1) and protein S6 kinase (p70S6K) [13]. Concomitantly, active mTORC1 prevents autophagy by phospho-inhibiting the UNC51-like kinase 1 (ULK1) at Ser757 that interacts with two partners: the autophagy related gene 13 (Atg13) and the FAK-family interacting protein of 200 kDa (FIP200). These three proteins form together the so-called ULK1 complex (Figure 1) [12, 14]. When mTORC1 is inhibited, ULK1 is activated and is able to phosphorylate Atg13 and FIP200. This is the first step that leads to the autophagosome formation (**Fig.1**) [12, 14, 15].

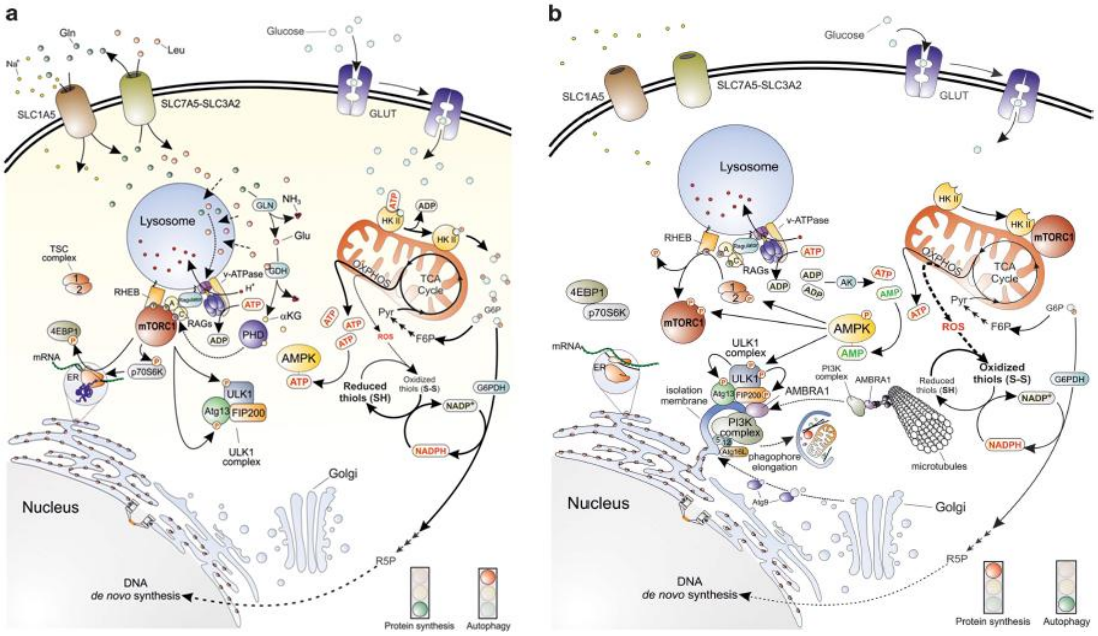


**Fig. 1** Cells coordinate energy and synthesis processes with the extracellular stimuli and amino acids and glucose availability**.** mTORC1is the unique molecular transducer of cellular needs**.** Once activated, mTORC1 activates protein synthesis by phosphorylating 4EBP1 and p70S6K, and concomitantly inhibits autophagy by phosphorylating ULK1 complex at the level of ULK1 and Atg13 [8].

In the last years a growing amount of evidence argues for the correlation between oxidative stress and autophagy [8].

Cells are always subjected to the effects of highly reactive oxidizing molecules thathave the ability to easily take electrons from cellular biomolecules and to trigger chain

reactions, leading to cell structure damage. The main classes of these molecules are reactive oxygen species (ROS) and reactive nitrogen species (RNS), endogenously produced at the highest concentration. It has been shown that ROS induce autophagy upon nutrient deprivation [16] and it is suggested by the evidence that antioxidant treatment prevents autophagy [17]. It has been proposed that the mitochondria represent the principal source of ROS required for autophagy induction [18, 19]; in fact, in lack of nutrients, the energetic stress increases ATP demand and causes mitochondrial overburden with an increasing ROS production. It could be possible that there is a factor which links mitochondria with the autophagic machinery. A hypothesis is that hexokinase II (HKII), the mitochondria-located enzyme responsible for the first step of glycolysis, binds to and inhibits mTORC1, loosing its ability to decrease ROS [20, 21, 22, 23].

AMPK could be another good candidate for a very fast induction of autophagy mediated by redox-sensitive proteins. Indeed, AMPK has been proposed to be activated by S-glutathionylation (formation of a mixed disulphide with GSH) of its reactive cysteines located at the α- (Cys299 and Cys304) and β-subunits (**Fig. 2**) [24, 25]. The thiol redox homeostasis is crucial in autophagy and it is supported by the evidence that just the chemically oxidation of GSH is able to induce autophagy even in the absence of any autophagic stimulus [16]. This assumption is according to the fact that many proteins involved in autophagy activation are rich in Cys residues [16]. Along this line, also p62 contains a zinc-finger motif (ZZ) rich in cysteine residues that that could be redox regulated.

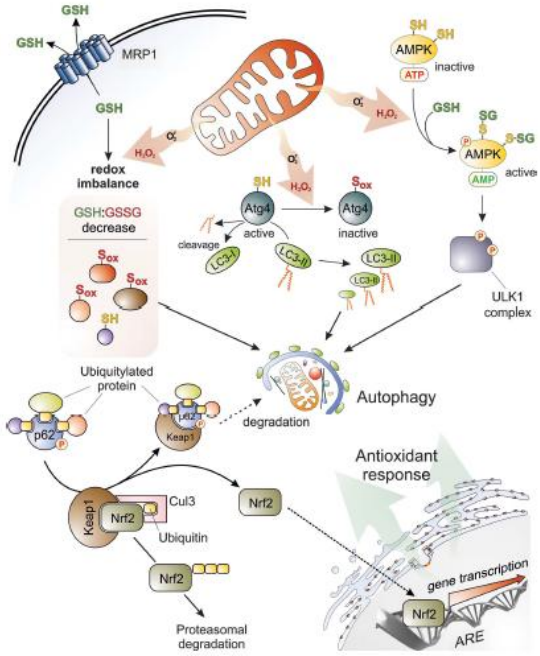


**Fig. 2** Importance of thiol redox homeostasis in autophagy . Ubiquitin-like systems Atg7-Atg3 and Atg7-Atg10, p62 and AMPK have cysteine residues that could be redox regulated [8]

Autophagy and ox-stress have been shown to be interconnected in a more intimate and coordinated maner. Particularly, in 2010, it was discovered that p62 can activate the antioxidant transcription factor Nrf2 (nuclear factor erythroid 2-related factor 2) (**Fig. 2**). In absence of stress conditions, Kelch-like ECH- associated protein 1 (Keap1), that is an adapter protein of the Cul3-ubiquitin E3 ligase complex, degrade Nrf2 [26, 27]. In case of redox imbalance, p62, when phosphorylated at Ser351, binds to aggregates of ubiquitylated proteins and increases its affinity for Keap1 (**Fig. 2**), inducing Keap1 degradation via autophagy [28, 29]. These events leave Nrf2 free to accumulate and translocate in the nucleus. Here, Nrf2 binds to the antioxidant-responsive elements (ARE) in the promoter regions of antioxidant and detoxifying genes [30], inducing their transcription (**Fig. 2**).

These evidences show that ROS and RNS are the upstream modulators of autophagy, that is required for the cell to simultaneously overcome starvation and oxidative stress

conditions. Therefore, any dysfunction in this regard has been found to be involved in the onset of pathological states [31, 32, 33].

## AIM OF THE PROJECT

The general aim of this work is to improve the knowledge of PD pathophysiology.

The first aim of this work was focused on the characterization of the presence of ox-stress in PD mouse model and in patients' cells.

The second aim was focused on the study of the effects of pharmacological manipulation of the ox-stress pathway to improve muscle pathology and ERT efficacy. We used antioxidants and drugs that are already known to improve the oxidative status of cells, and evaluate their effects on disease pathology and clinical course of the disease.

## RESULTS

- **microRNA implicated in ox-stress or disregulated in PD mice.**

We analyzed miRNA expression profiles in tissues from PD mice with the aim to identify "disease-specific" miRNAs for PD (see 3$^{rd}$ part of this thesis). The analysis was performed in quadriceps, a tissue which is relevant for PD, on 3 months old mice by using a NextGeneration Sequencing (NGS) approach. The NGS analysis generated a list of differentially expressed miRNAs in a tissue which represents one of the primary target organs of PD. Interestingly, in the PD mouse muscle we found a deregulation of some miRNAs (**Table 1**). Some miRNA that are known to modulate target genes

involved in oxidative stress, autophagy and inflammation result to be differentially expressed in PD mouse muscle (**Fig. 3**).

| Deregulation of microRNA associated with oxidative stress and autophagy in PD mouse muscle | | |
|---|---|---|
| **miRNA ID** | **Trend in PD mice** | **Target Genes** |
| miR-142-5p | upregulated | NRf2 |
| miR-34c | upregulated | p53, Bcl2 |
| miR-145 | upregulated | BNIP3 |
| Let-7 family | upregulated | ARG2, Bach1 |
| miR-144 | downregulated | mTOR, Nrf2 |
| miR-451 | downregulated | AKT, FoxO3a |
| miR-30a | downregulated | Beclin |
| miR-181a | downregulated | Atg5 |

**Fig. 3** MicroRNAs associated with oxidative stress that are dysregulated in PD mouse model.

- **Patients' fibroblasts and GAA KO mice show increased ox-stress.**

Since free radicals and resulted products can be used as biomarkers of oxidative stress, we performed a Thiobarbituric Acid Reactive Substances (TBARS) to measure the amount of lipid peroxidation products using thiobarbituric acid as a reagent.We measured lipid peroxidation levels in homogenates from 3-months-old WT and KO PD mice (gastrocnemius, quadriceps, liver, heart, diaphram). The TBARS experiment has been performed also on fibroblasts isolated from patients. As shown in **Fig.4**, a significant increase was observed in the 4 muscles of PD mice compared to WT mice and in patients' fibroblasts compared to control fibroblasts, suggesting the presence of oxidative stress in PD tissues and cells. The finding of minor increases in the liver suggested that the deregulation of the redox state is a typical feature of muscular tissues in PD, as expected in a metabolic myopathy such as PD [34].

We also analyzed the intracellular ROS levels in 3 months PD mice and in fibroblasts isolated from patients and controls (**Fig. 4A**). DCFDA assay uses the cell permeant reagent 2',7' –dichlorofluorescin diacetate (DCFDA), a fluorogenic dye that measures hydroxyl, peroxyl and other reactive oxygen species (ROS) activity within the cell. We used cells and tissue homogenates to evaluate ROS levels. We found that in all the muscles analyzed, as well as in patients' fibroblasts, a strong increase in ROS levelswas observed with respect to control samples. These data are in line with those obtained for lipid peroxidation.

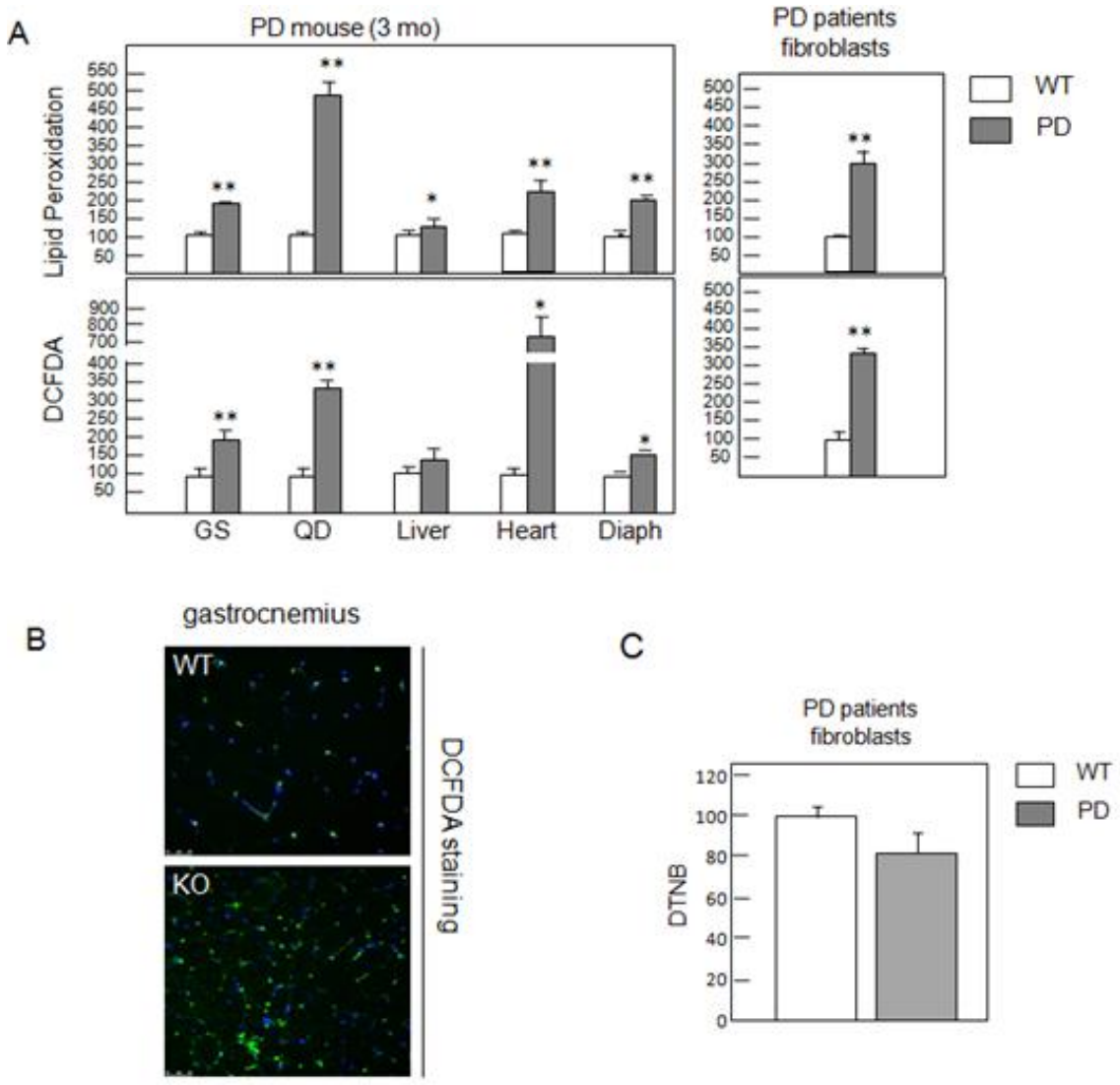


**Fig. 4 A )**Lipid peroxidation and ROS production in 3 months PD mice and fibroblasts isolated from patients. Lipid peroxidation levels determined by TBARS assay in homogenates from different tissues in WT (white bars) and in PD samples (grey bars); intracellular ROS levels were determined by DCFDA assay. * *p < 0.05, ** p<0.01.* ***B)*** DCFDA staining in GAA WT e KO mice gastrocnemius. The results show a major amount of ROS in GAA KO mice than in GAA WT mice. Data shown are the means ± S.D. of three independent experiments.**C)** DTNB on PD and control fibroblasts. Results show a reduction of sulfhydryl groups, related to oxidative stress conditions, in PD fibroblasts compared to control fibroblasts.

To validate these data we also performed a DCFDA staining in GAA WT and KO gastrocnemius (**Fig. 4B**) that confirms icreased ROS in GAA KO mice compared to WT mice.

We used Ellman's reagent (5,5'-dithiobis-2-nitrobenzoic acid or DTNB) which is a chemical used to quantify the sulfhydryl group of GSH in the cells. The thiol redox

homeostasis depends on the redox state of the cell. Results show a reduction of sulfhydryl groups, related to oxidative stress conditions, in PD fibroblasts compared to control fibroblasts (**Fig. 4C**).

We next analyzed the expression of proteins involved in oxidative stress cascade by western blotting analysis in PD fibroblasts and muscles. MAPKs are a family of evolutionarily highly conserved enzymes that manage the response to growth stimulatory signals, such as insulin or epidermal growth factor (EGF), as well as adverse signals, such as cytotoxic and genotoxic substances. They include extracellular signal–regulated kinases (ERKs), stress-activated protein kinases, also known as c-jun N-terminal kinases (SAPK ⁄JNKs), and the p38-MAPKs (**Fig. 5**). Activation of these pathways is not unique to oxidative stress, as they are known to have central roles in regulating cellular responses to other stresses as well as regulating normal growth and metabolism. Indeed, in some situations the response to oxidants may involve overstimulation of normal ROS-regulated signalling pathways. In general, the heat shock response, ERK pathway exerts a pro-survival influence during oxidant injury, whereas activation p38 are more commonly linked to apoptosis [35]. Oxidants seem to activate the ERK, mimicking the actions of growth-factors [36, 37]. Oxidative stress might induce activation of the JNK and p38 kinase pathways by an additional mechanism. The redox regulatory protein thioredoxin (Trx) has been shown to activate an upstream factor of both JNK and p38, which is inhibited under normal conditions [38].

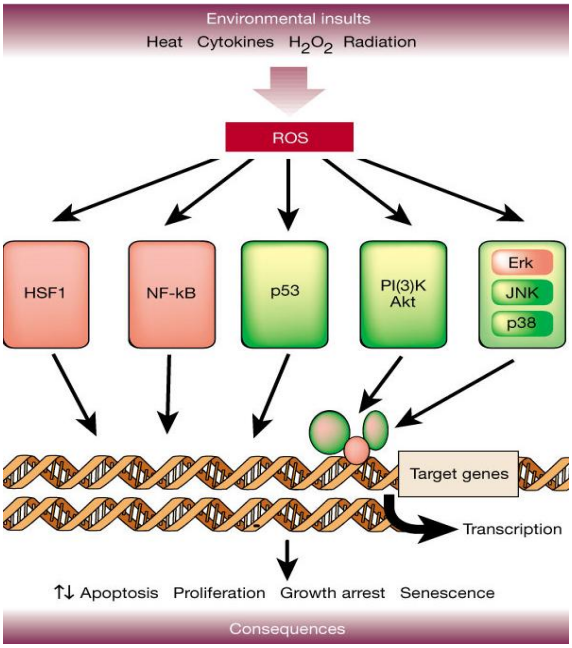


**Fig. 5** ROS can originate outside the cell, or may be generated intracellularly in response to external stimuli. PI(3)K/Akt and MAPK pathways regulate transcription factors through phosphorylation. The consequences of the response vary widely, with the ultimate outcome being dependent on the balance between these stress-activated pathways.

We analyzed the phosphorylation levels of p38 and ERK1/2 by western blots in human fibroblasts. This analysis confirmed that increased oxidative stress was present in PD patients (**Fig. 6**).

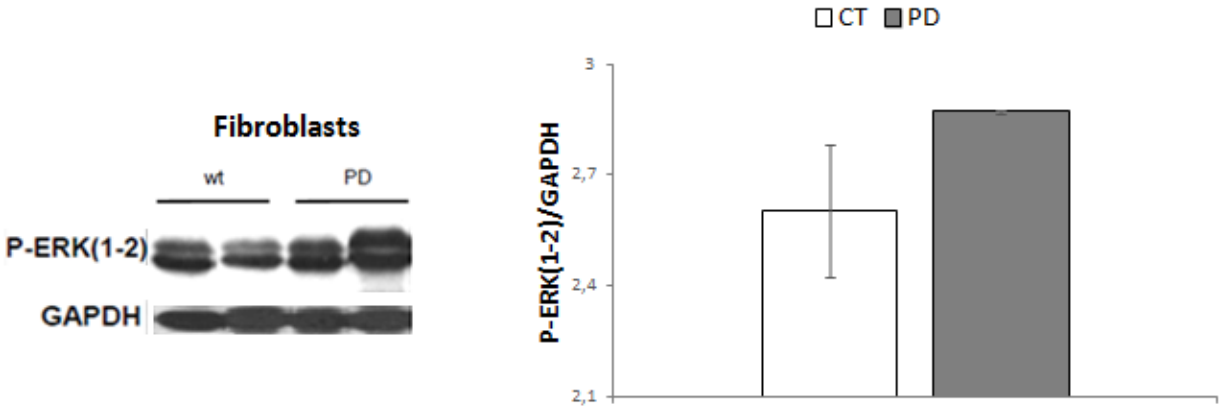


**Fig.6** Western blot analysis of P-ERK (1-2) in WT and PD fibroblasts. P-ERK (1-2) seem to be more abundant in PD fibroblast compared to control.

Western blots analysis in gastrocnemii from WT and KO mice showed increased phosphorylation levels of p38 and ERK1/2 in PD mice than in control mice. This result was particularly evident in heart (**Fig. 7**).

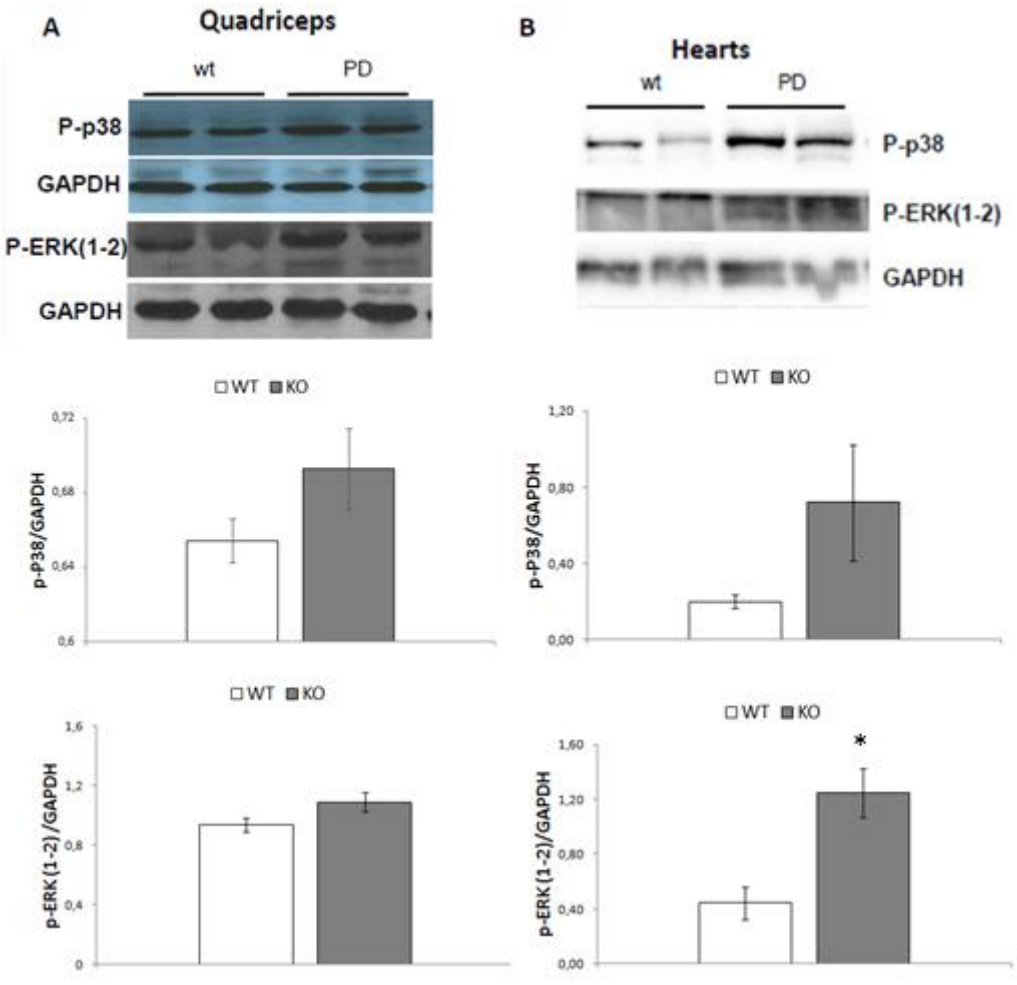


**Fig. 7** Expression of genes involved in ox-stress in 3 months PD mice. Western blots of homogenates from quadriceps and hearts in wt and PD mice.* *p < 0.05.*

We also analyzed autophagic markers, such as MAP-LC3 and p62. Microtubule-associated proteins LC3 (MAP-LC3, herein named LC3) is the major constituent of the autophagosome and is widely used as indicators of autophagy, whereas p62 is an ubiquitin binding protein whose degradation is directly related to autophagosomesclearance. We observed the appearance of LC3-II in the PD samples,

indicating that autophagy wasinduced, but, at the same time, we found an increase in p62 levels (**Fig.8**).

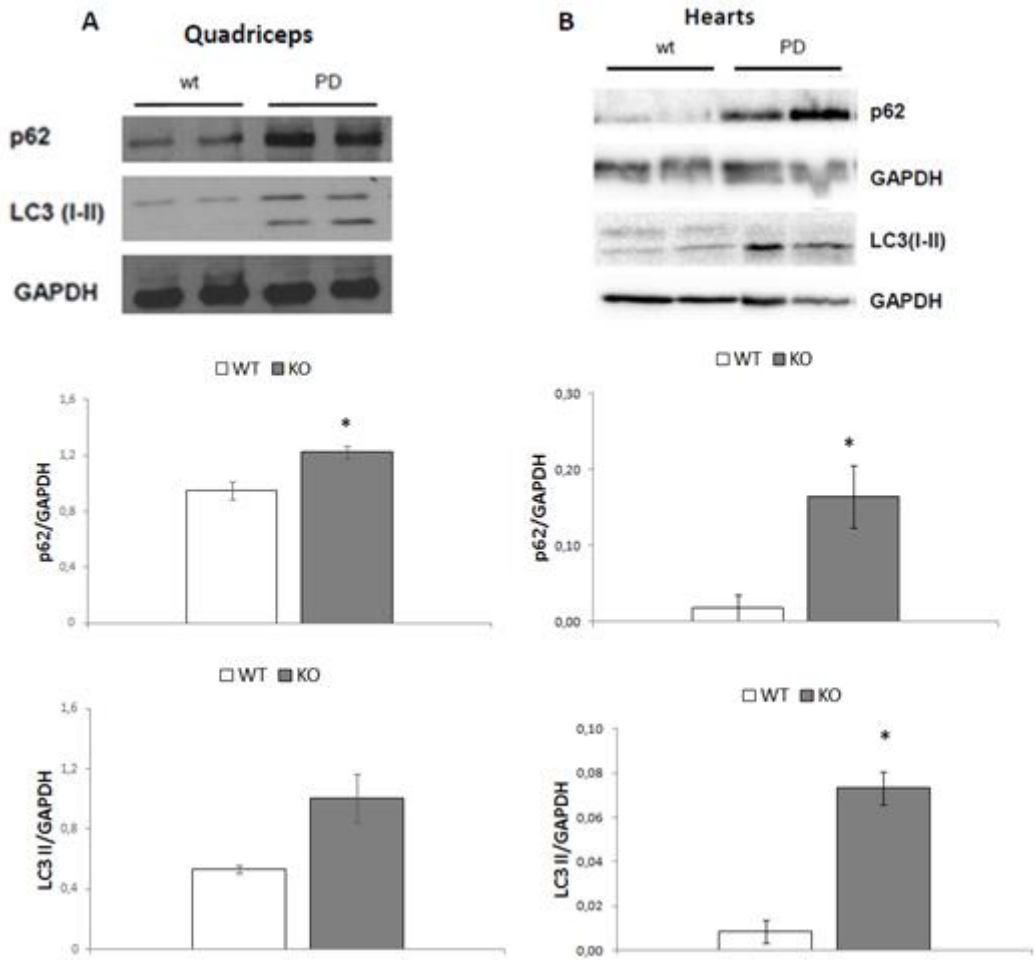


**Fig. 8** Expression of genes involved in autophagy in 3 months PD mice. Western blots of homogenates from quadriceps (A) and heart (B) in wt and PD mice. Densitometric analyses are reported below images.* *p < 0.05*

- **Effects of ERT and drugs on oxidative stress.**

We next studied the effects of ERT on the levels of ox-stress. First of all, we tested whether ERT could rescue oxidative stress in PD patients. The results of TBARS and DCFDA assays on homogenates from 3 months GAA WT and KO mice suggest an improvement of oxidative stress levels after ERT treatment in all muscles (**Fig. 9**).

Results are different in the liver, in which ERT have no effect on oxidative stress. This result is consistent with the minor increase of ox-stress in PD liver compared to other organs.

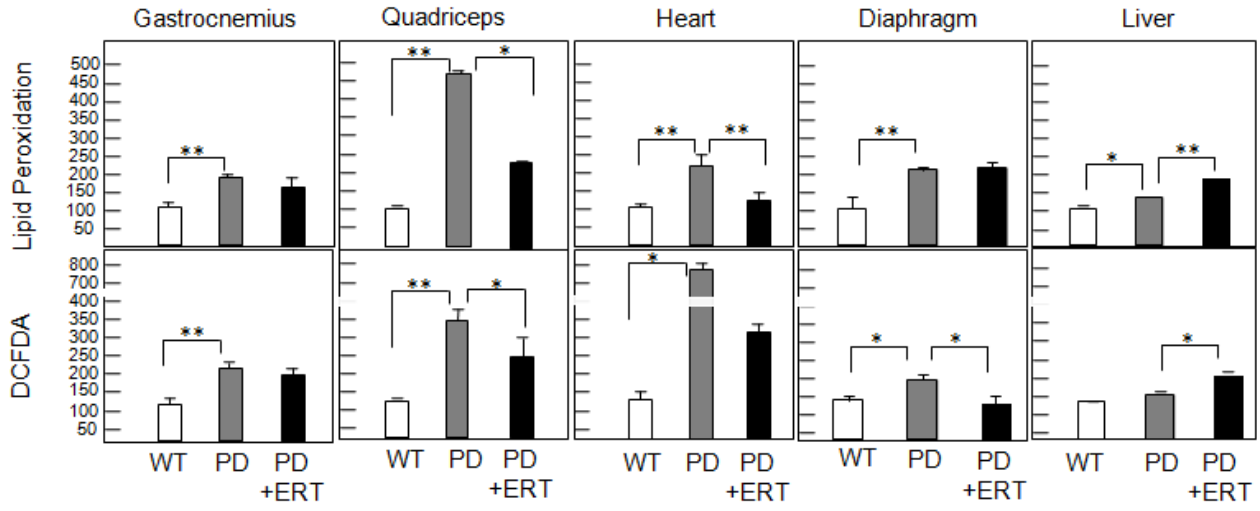


**Fig. 9** TBARS and DCFDA assays on homogenates from 3 months GAA WT and KO mice suggest an improving of oxidative stress conditions after ERT treatment .* *p < 0.05, ** p<0.01*

Albeit not statistically significant, the analysis by western blot of phosphorylated ERK and p38 proteins in quadricepts and hearts of 3 months WT and KOmice shows the same trend of previous experiments (**Fig. 10**).

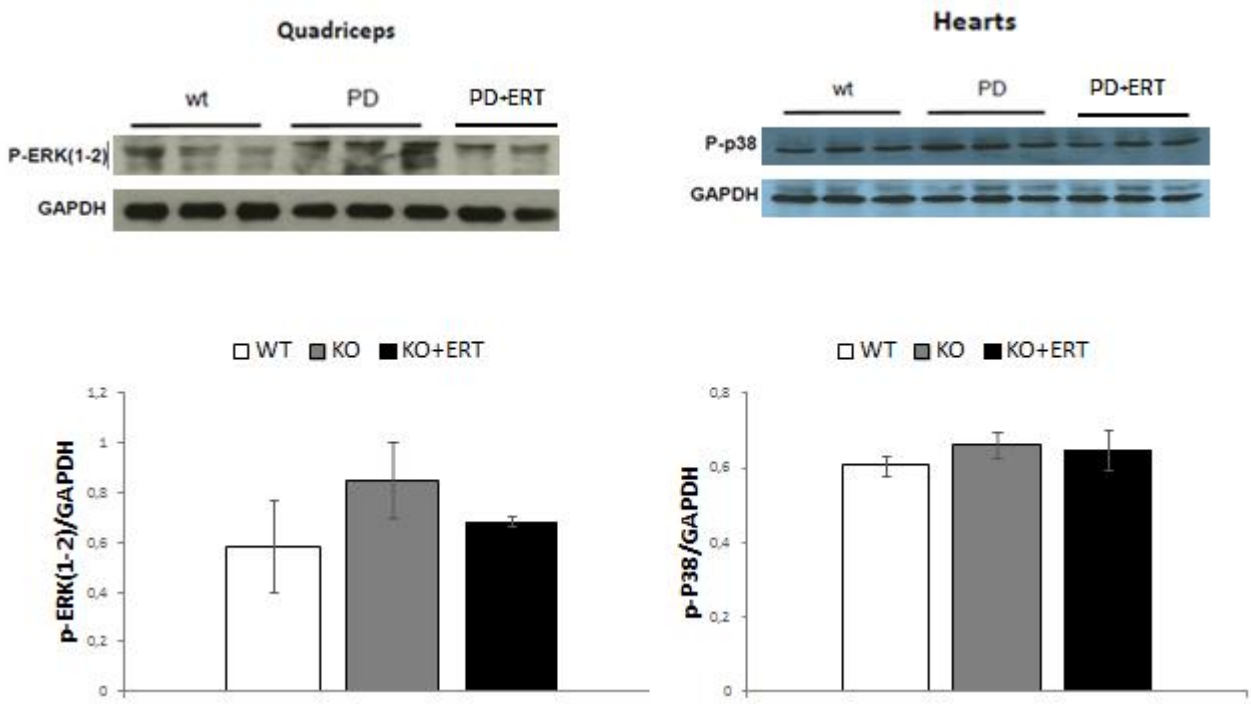


**Fig. 10** Western blot analysis on quadriceps and hearts from 3 months GAA WT, KO andKO + ERT mice suggest an improving of oxidative stress conditions after ERT treatment .

We also investigated the effect of known antioxidants on oxidative stress in PD cells. Cells were treated with C001 100 µM for 24 hours and analyzed for TBARS and DCFDA assays. The results showed a more evident decrease of ROS and lipid peroxidation in PD fibroblasts after the treatment with ascorbic acid than in control fibroblasts (**Fig. 11**).

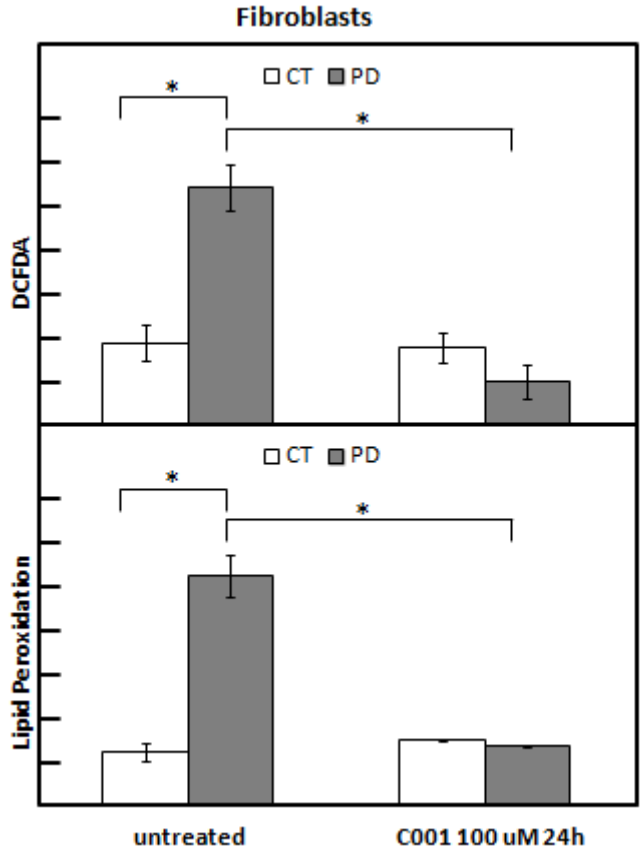


**Fig. 11** TBARS and DCFDA assays on PD and control fibroblasts. Results show a significant decrease of ROS and lipid peroxidation in PD fibroblasts after a 24 hours treatment with C001.* $p < 0.01$

Gastrocnemii and hearts from WT and GAA KO mice were treated with 3 g/kg with a second compound (C002) and ox-stress levels were evaluated by TBARS and DCFDA assays. Results showed significant decrease of ox-stress levels in PD mice treated with C002, compared to untreated KO mice (**Fig. 12**).

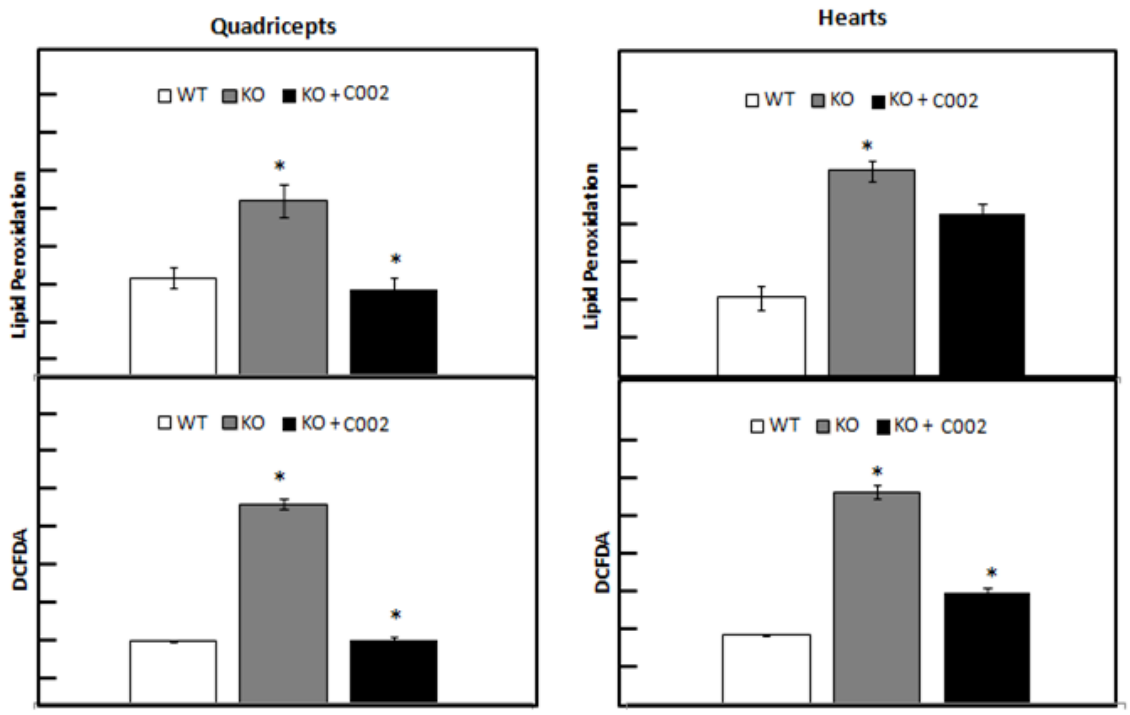


**Fig. 12** TBARS and DCFDA assays on gastrocnemius and hearts from WT and GAA KO mice treated with C002 3 mg/kg. Results show a significant decrease of ROS and lipid peroxidation in treated PD mice, compared to untreated. * *p < 0.01*

Furthermore, we investigated about the possible effect of C002 on the efficacy of ERT in vitro. We observed an increase rhGAA activity and stability in PD fibroblasts treated with C002, compared to untreated, shown by GAA activity assay and western blot analysis (**Fig. 13**).

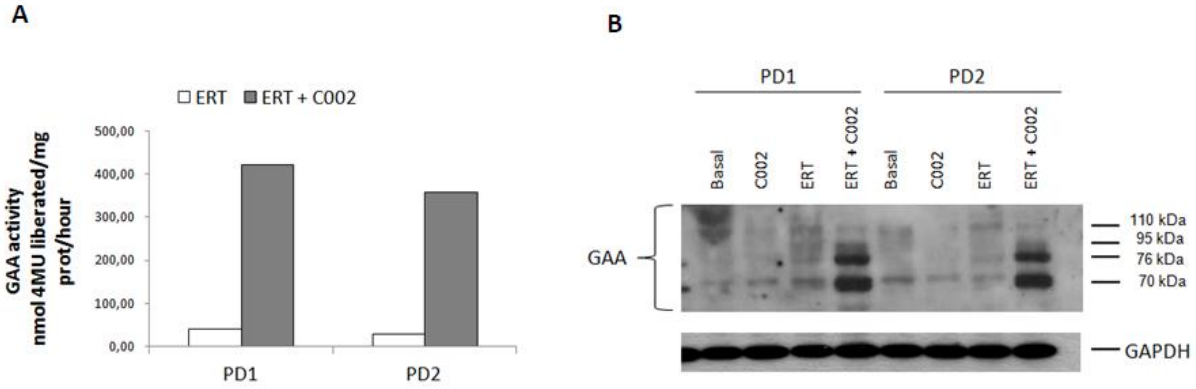


**Fig. 13 A)** Percent of GAA activity increasing in PD fibroblasts treated with ERT with and without C002. The anti-oxidant increase rhGAA activity in cells, probably improving its stability in cells **B).**

## METHODS

A KO Pompe disease mouse model obtained by insertion of neo into the *GAA* gene exon 6 Raben et al, [1998] was purchased from Charles River Laboratories (Wilmington, MA), and is currently maintained at the Cardarelli Hospital's Animal Facility (Naples, Italy). Animal studies were performed according to the EU Directive 86/609, regarding the protection of animals used for experimental purposes. Every procedure on the mice were performed with the aim of ensuring that discomfort, distress, pain, and injury would be minimal. Mice were euthanized following anesthesia. Human PD fibroblasts (approximately 30 cell lines) are already available at the cell bank of the Department of Translational Medical Sciences (DISMET), Section of Pediatrics, Federico II University, Naples.

*In vivo experiments*

Mice were injected into the retroorbital vein with rhGAA at a dose of 40 mg/kg. The animals were killed after 24 hours, the different tissue were harvested, homogenized and lysated. Each group of mice was composed of three 12-week-old animals.

*Cell Culture*

Fibroblasts from control individuals and from PD patients were obtained from the cell repository at the Department of Traslational Medicine, Università degli Studi di Napoli Federico II. Fibroblasts were grown in DMEM medium supplemented with fetal bovine serum, L-glutamine and antibiotics. Cells were incubated with rhGAA at 50 ng/ul for 6 hours and with Ascorbic Acid 100 uM for 24 hours.

*Western Blot*

PD and control fibroblasts and mice tissue protein extracts were obtained by lysing cells with RIPA Buffer and protease inhibitors for 3 minutes at 50 oscillations/minute in tissue lyser and by five cycles of freeze-thawing. Samples were centrifuged at 13000 rpm for 30 minutes at 4°C. The supernatant constituted the protein extract. Fibroblast and tissues extracts were subjected to sodium dodecyl sulfate polyacrylamide gel electrophoresis (7 or 10% acrylamide in different experiments) and proteins were transferred to nitrocellulose membrane (Millipore, Billerica, MA). Immunoreactive proteins were detected by chemiluminescence (ECL, Amersham, Freiburg, Germany). Quantitative analysis of band intensity was performed using ImageJ.

*DCFDA assay*

Todetermine the ROS levels within the cytosol, cells were incubated with cell permeable, redox-sensitive fluorophore 2',7'-dichlorodihydrofluorescein diacetate (H2-DCFDA, Sigma-Aldrich) at the concentration of 20 μMfor30 min at 37 °C. Cells were then washed with warm PBS supplemented with 1 mM CaCl2, 0.5 mM MgCl2, 30 mMglucose (PBS plus) 2 times, detached by trypsin, centrifuged at 1000 g for 10 min and resuspended in PBS plus at a cell density of 1x105cells/ml. After diffusion in to the cell, DCFDA is deacetylated by cellular esterases to a non-fluorescent compound, which is later oxidized by ROS into 2', 7' –dichlorofluorescein (DCF). DCF is a highly fluorescent compound which can be detected by fluorescence spectroscopy with maximum excitation and emission spectra of 495 nm and 529 nm respectively using a Perkin-Elmer LS50 spectrofluorimeter. Emission spectra were acquired at a scanning speed of 300 nm/min, with 5 slitwidths for excitation and emission. ROS production was expressed as percentage of DCF fluorescence intensity of the sample under test, with respect to the untreated sample. Three separate analyses

were carried outin triplicate with each extract. Control experiments were performed by supplementing cell cultures with identical volumes of DMSO.

*TBARS assay*

The levels of lipid peroxidation were determined by using the thiobarbituric acid (TBA) reactive substances (TBARS) assay. Since TBA reacts with oxidative degradation products of lipids, and complexes absorb at 532 nm, this assay was used to determine lipid peroxidation levels. At the end of the experiment, cells were detached by trypsin, centrifuged at 1,000 g for 10 min and $5x10^5$ cells were resuspendend in ice cold PBS and mixed with 0.67% TBA and an equal volume of 20% trichloroacetic acid. Samples were then heated at 95 °C for 30 min, incubated on ice for 10 min and centrifuged at 3,000g for 5 min, at 4 °C. Samples were read at 532 nm.

*DTNB assay*

To estimate intracellular GSH levels, the interaction of the sulfhydryl group of GSH with 5,5'-dithiobis-2-nitrobenzoic acid (DTNB) was used. DTNB produces a yellow-coloured compound, 5-thio-2-nitrobenzoic acid (TNB), whose intensity can be measured at 412 nm. Thus, the rate of TNB production is directly proportional to the concentration of GSH in the sample. At the end of the experiment, cells were detached by trypsin, centrifuged at 1000 g for 10 min and resuspendend in lysis buffer (300 mM NaCl, 0.5% NP-40 in 100 mM TrisHCl, pH7.4) containing protease inhibitors. After 30 min incubation on ice, lysates were centrifuged at 14,000 g for 30 min at 4 °C. Supernatant protein concentration was determined by Bradford assay. Then, 50 µg of proteins were incubated with 3 mM EDTA, 144 µM DTNB in 30 mM TrisHCl pH 8.2, centrifuged at 14,000g for 5 min at RT and the absorbance of

the supernatant was measured at 412 nm using a multiplate reader (Biorad). The intracellular GSH level determined using a reference curve obtain by GSH as a standard (1-500 µl). GSH levels were expressed as percentage of TNB absorbance of the sample under test, with respect to the untreated sample. Three separate analyses were carried out with each extract. Control experiments were performed by supplementing cell cultures with identical volumes of DMSO.

*DCFDA staining*

Gastrocnemii from WT and KO mice were dissected and frozen in isopentane in liquid nitrogen. Then they were cut in 10 µm thick tissue sections using a cryostat and were mounted onto histological slides. Slides were dried for 30 minutes at room temperature and incubated with DCFDA 10 µM in PBS for 15 minutes. After 3 washing step with PBS, tissues were analyzed by fluorescence microscopy.

*GAA activity assay*

GAA activity was assayed by using the fluorogenic substrate 4-methylumbelliferyl-α-D-glucopyranoside (Sigma-Aldrich). Briefly, 25 µg of protein were incubated with the fluorogenic substrate (2mmol/l) in 0,2 mol/l acetate buffer, pH 4.0, for 60 minutes in incubation mixtures of 20 µl. The reaction was stopped by adding 1 ml of glycine-carbonate buffer, pH 10.7. Fluorescence was read at 365 nm (excitation) and 450 nm (emission) on a Turner Biosystem Modulus fluorometer.

## CONCLUSIONS

PD pathophysiology and its molecular/cellular mechanisms are not fully understood. It has been shown that a failure of productive autophagy in muscle tissue contributes strongly to disease pathology in PD patients [1] and would interfere with the correct delivery of recombinant enzyme [1, 4]. Improving therapy is an urgent need, so our study is focused on study the autophagy impairment in PD and the mechanisms that could lead to this alteration. The strong correlation between oxidative stress and autophagyhas been fully elucidated. In addition, it has been found that PD mice and humans show multiple mitochondrial defects, a profound dysregulation of $Ca^{2+}$ homeostasis and an increase in reactive oxygen species [7].

In line with this evidences we investigated about the presence of ox-stress in GAA KO mouse muscles and PD patients fibroblasts, and we decided to screen already known drugs to improve the oxidative status of cells and evaluate their effects on disease pathology. Our data confirmed increasing ox-stress in PD mice tissue (in particular, in muscle tissues, as expected) and in patients' fibroblasts, compared to controls, by TBARS, DCFDA and DTNB assay. Western blot analysis of ox-stress markers on mice tissue and patients' fibroblasts also confirmed the same evidence.

A very interesting data was the positive effect of ERT on ox-stress in muscle tissue from PD mice observed by biochemical assays and western blot analysis, even if the reason of this effect is not completely clear. Furthermore, when we have treated KO mice and PD fibroblasts with antioxidants, we observed a significant improvement of rhGAA activity. This data open the way to other answer about the link between autophagy impairment and oxidative stress. Our next step is understanding the molecular mechanisms underlying this connection and how we can modulate autophagy and ox-stress pathways as new therapeutic target. Moreover, the use of drugs already on the

market could make easier to start new therapeutic approaches in patients. Therefore, the connection between autophagy and ox-stress can be the key to better understand PD pathophysiology and to address a novel therapeutic approach.

## BIBLIOGRAPHY

[1] Shea L, Raben N (2009). Autophagy in skeletal muscle: implications for Pompe disease. *Int J Clin Pharmacol Ther***47** Suppl 1: S42–47

[2] Fukuda T, Ahearn M, Roberts A, Mattaliano RJ, Zaal K, Ralston E, Plotz PH, Raben N.Autophagy and mistargeting of therapeutic enzyme in skeletal muscle in Pompe disease Mol Ther. 14, 831-9 (2006)

[3] Spampanato C, Feeney E, Li L, Cardone M, Lim JA, Annunziata F, Zare H, Polishchuk R, Puertollano R,Parenti G, Ballabio A, Raben N. Transcription factor EB (TFEB) is a new therapeutic target forPompe disease. EMBO Mol Med. 5, 691-706(2013).

[4] Fukuda T, Ewan L, Bauer M, Mattaliano RJ, Zaal K, Ralston E, et al. Dysfunction of endocytic and autophagic pathways in a lysosomal storage disease. Ann Neurol. 2006b;59:700–708.

[5] Villani GR1, Di Domenico C, Musella A, Cecere F, Di Napoli D, Di Natale P. Mucopolysaccharidosis IIIB: oxidative damage and cytotoxic cell involvement in the neuronal pathogenesis.Brain Res. 2009 Jul 7;1279:99-108

[6] Vázquez MC1, Balboa E, Alvarez AR, Zanlungo S. Oxidative stress: a pathogenic mechanism for Niemann-Pick type C disease.Oxid Med Cell Longev. 2012;2012:205713.

[7] Jeong-A Lim, Lishu Li, Or Kakhlon, Rachel Myerowitz and Nina Raben. Defects in calcium homeostasis and mitochondria can be reversed in Pompe disease.Autophagy 2015 Feb; 11(2): 385–402.

[8] G Filomeni, D De Zio and F Cecconi. Oxidative stress and autophagy: the clash between damage and metabolic needs. Cell Death Differ. 2015 Mar; 22(3): 377–388.

[9] Martina JA, Diab HI, Brady OA, Puertollano R. TFEB and TFE3 are novel components of theintegrated stress response. EMBO J. 35, 479-95(2016)

[10] Mizushima N. The pleiotropic role of autophagy: from protein metabolism to bactericide. Cell Death Differ. 2005;12(Suppl 2):1535–1541.

[11] Kroemer G, Marino G, Levine B. Autophagy and the integrated stress response. Mol Cell. 2010;40:280–293

[12] Yang Z, Klionsky DJ. Mammalian autophagy: core molecular machinery and signaling regulation. Curr Opin Cell Biol. 2010;22:124–131.

[13] Neufeld TP. Autophagy and cell growth—the yin and yang of nutrient responses. J Cell Sci. 2012;125:2359–2368.

[14] Nazio F, Cecconi F. mTOR AMBRA1, and autophagy: an intricate relationship. Cell Cycle. 2013;12:2524–2525

[15] Fimia GM, Di Bartolomeo S, Piacentini M, Cecconi F. Unleashing the Ambra1-Beclin 1 complex from dynein chains: Ulk1 sets Ambra1 free to induce autophagy. Autophagy. 2011;7:115–117.

[16] Filomeni G, Desideri E, Cardaci S, Rotilio G, Ciriolo MR. Under the ROS. thiol network is the principal suspect for autophagy commitment. Autophagy. 2010;6:999–1005.

[17] Levonen AL, Hill BG, Kansanen E, Zhang J, Darley-Usmar VM. Redox regulation of antioxidants, autophagy, and the response to stress: Implications for electrophile therapeutics. Free Radic Biol Med. 2014;71C:196–207

[18] Murphy MP. How mitochondria produce reactive oxygen species. Biochem J. 2009;417:1–13

[19] Scherz-Shouval R, Z. Elazar. ROS, mitochondria and the regulation of autophagy. Trends Cell Biol. 2007;17:422–427.

[20] Roberts DJ, Tan-Sah VP, Ding EY, Smith JM, Miyamoto S. Hexokinase-II positively regulates glucose starvation-induced autophagy through TORC1 inhibition. Mol Cell. 2014;53:521–533.

[21] da-Silva WS, Gomez-Puyou A, de Gomez-Puyou MT, Moreno-Sanchez R, De Felice FG, de Meis L, et al. Mitochondrial bound hexokinase activity as a preventive antioxidant defense: steady-state ADP formation as a regulatory mechanism of membrane potential and reactive oxygen species generation in mitochondria. J Biol Chem. 2004;279:39846–39855.

[22] Wang RC, Wei Y, An Z, Zou Z, Xiao G, Bhagat G, et al. Akt-mediated regulation of autophagy and tumorigenesis through Beclin 1 phosphorylation. Science. 2012;338:956–959.

[23] Oude Ophuis RJ, Wijers M, Bennink MB, van de Loo FA, Fransen JA, Wieringa B, et al. A tail-anchored myotonic dystrophy protein kinase isoform induces perinuclear clustering of mitochondria, autophagy, and apoptosis. PLoS One. 2009;4:e8024.

[24] Cardaci S, Filomeni G, Ciriolo MR. Redox implications of AMPK-mediated signal transduction beyond energetic clues. J Cell Sci. 2012;125:2115–2125

[25] Zmijewski JW, Banerjee S, Bae H, Friggeri A, Lazarowski ER, Abraham E. Exposure to hydrogen peroxide induces oxidation and activation of AMP-activated protein kinase. J Biol Chem. 2010;285:33154–33164

[26] Komatsu M, Kurokawa H, Waguri S, Taguchi K, Kobayashi A, Ichimura Y, et al. The selective autophagy substrate p62 activates the stress responsive transcription factor Nrf2 through inactivation of Keap1. Nat Cell Biol. 2010;12:213–223.

[27] Lau A, Wang XJ, Zhao F, Villeneuve NF, Wu T, Jiang T, et al. A noncanonical mechanism of Nrf2 activation by autophagy deficiency: direct interaction between Keap1 and p62. Mol Cell Biol. 2010;30:3275–3285.

[28] Ichimura Y, Waguri S, Sou YS, Kageyama S, Hasegawa J, Ishimura R, et al. Phosphorylation of p62 activates the Keap1-Nrf2 pathway during selective autophagy. Mol Cell. 2013;51:618–631.

[29] Taguchi K, Fujikawa N, Komatsu M, Ishii T, Unno M, Akaike T, et al. Keap1 degradation by autophagy for the maintenance of redox homeostasis. Proc Natl Acad Sci USA. 2012;109:13561–13566.

[30] Ma Q. Role of nrf2 in oxidative stress and toxicity. Annu Rev Pharmacol Toxicol 2013; 53:401–426.

[31] Liang C, Feng P, Ku B, Dotan I, Canaani D, Oh BH, et al. Autophagic and tumour suppressor activity of a novel Beclin1-binding protein UVRAG. Nat Cell Biol. 2006;8:688–699.

[32] Karantza-Wadsworth V, Patel S, Kravchuk O, Chen G, Mathew R, Jin S, et al. Autophagy mitigates metabolic stress and genome damage in mammary tumorigenesis.

[33] Takamura A, Komatsu M, Hara T, Sakamoto A, Kishi C, Waguri S, et al. Autophagy-deficient mice develop multiple liver tumors. Genes Dev. 2011;25:795–800.

[34] Parenti G, Andria G.Pompe disease: from new views on pathophysiology to innovative therapeutic strategies. Curr Pharm Biotechnol. 2011 Jun;12(6):902-15.

[35] Toren Finkel & Nikki J. Holbrook. Oxidants, oxidative stress and the biology of ageing. Nature 408, 239-247 (9 November 2000)

[36] Sachsenmaier, C. et al. Involvement of growth factor receptors in the mammalian UVC response. Cell 78, 963– 972 (1994).

[37] Wang, X. , McCullough, K. D. , Franke, T. F. & Holbrook, N. J. Epidermal growth factor receptor-dependent Akt activation by oxidative stress enhances cell survival. J. Biol. Chem. 275, 14624–14631 (2000).

[38] Saitoh, M. et al. Mammalian thioredoxin is a direct inhibitor of apoptosis signal-regulating kinase (ASK) 1. EMBO J. 17, 2596– 2606 (1998).

# Chapter 3

## microRNA as biomarkers in Pompe Disease

## INTRODUCTION

Assessing patient conditions and response to ERT is a critical issue in the management of this disorder. A major challenge, in this respect, is the need for reliable, measurable and objective markers of disease that are not influenced by inter and intra-investigator variance. While objective clinical measures for evaluating cardiac manifestations are available, the degree of muscle involvement remains difficult to assess. Currently, clinical tests (muscle strength, muscle function, patient-reported outcomes) are in common use to this purpose [1]. Although several of these tests have been specifically validated for PD [2, 3], some of them appear to be specific for subsets of patients, require specific medical skills and collaboration of patients. Key factors in the evaluation of these tests are their clinical relevance and the minimal clinically important difference, that for some of these tests needs to be further established [1]. Biochemical or imaging-based tests include the evaluation of the glucose tetrasaccharide (GLC4) [4] in plasma and urine, muscle ultrasound [5], muscle NMR [6]. Also in these cases, however, the clinical relevance of the tests needs further assessment.

The availability of reliable tests appears even more important for the development of guidelines for patient monitoring, for ERT inclusion and exclusion criteria that are currently being defined in many countries [such as UK, and other European countries; see EPoC criteria]. A set of reliable clinical and biochemical tests may also prove to be useful in optimizing ERT, and may in principle translate into economical benefits. They may also be precious tools in evaluating the efficacy of novel treatments or treatment protocols in comparison with existing therapies.

In addition disease markers that provide information on PD pathophysiology may allow for identification of new therapeutic targets and, possibly, for development of novel therapeutic strategies.

We explored the possibility to exploit microRNAs (miRNAs) as markers of disease in PD. miRNAs are a small non-coding RNAs that regulate gene expression by targeting messenger RNAs. miRNAs are able to concurrently target multiple effectors of pathways in the context of a network, thereby finely regulating multiple cellular functions involved in disease development and progression [7,8, 9].

In several other disease conditions, including muscular dystrophies [10] miRNA profiles have provided a read-out of altered pathways in response to disease [11], and have indicated potential targets of therapeutic intervention. In this respect, miRNAs have a great potential as diagnostic, prognostic and predictive disease biomarkers. Obtaining indirect read-outs of pathological processes is particularly important for certain disorders, such as PD, in which direct access to the affected tissue for molecular analyses would require invasive procedures (muscle biopsy).

In this study we analyzed the expression of miRNAs by a methodology based on Next-Generation Sequencing (NGS) and bioinformatic analysis in the PD murine model (muscle and heart), and in patients' plasma, in order to provide an additional measure to assess patients clinical conditions and response to treatments.

## RESULTS

- **The PD mouse model shows differential expression of miRNAs in gastrocnemius and heart.**

miRNAs expression profiles were analyzed by NGS in the mouse model of PD in comparison to wild-type animals. The analysis was performed in two tissues that are particularly relevant for the disease, heart and gastrocnemius, from PD mice and age-

matched wild-type mice. The tissues were collected at different time-points (3 and 9 months) that reflect different stages of disease progression and severity (**Fig. 1**).

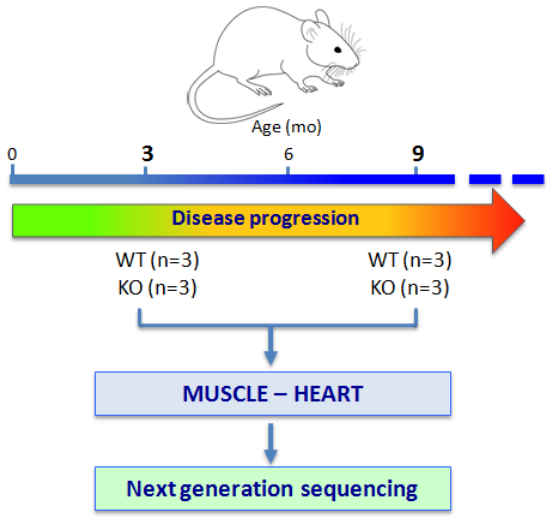


**Fig. 1** Experiment plan of NGS analysis in the mouse model of PD in comparison to wild-type animals.

After sample collection and small-RNA sequencing, a bioinformatic analysis was performed in order to assess reliability and statistical relevance of data. The threshold value for significance used to define up-regulation or down-regulation of miRNAs was a False Discovery Rate (FDR) < 0.05. The NGS analysis generated a list of differentially expressed miRNAs (DE-miRNA) in the tissues examined. We identified 198 miRNAs differentially expressed with statistical significance in gastrocnemius (**Fig. 2A**, left). Fifty-five miRNAs were differentially expressed at 3 months, 58 at 9 months, 85 were differentially expressed at both ages. We also found 66 DE-miRNAs in heart (**Fig. 2A**, right): 17 miRNAs were differentially expressed at 3 months and 44 at 9 months; 5 miRNAs were differentially expressed at both ages in heart.

DE-miRNAs were either up-regulated or down-regulated. In gastrocnemius 98 miRNAs were down-regulated and 100 up-regulated, while in heart 31 miRNAs were down-regulated and 35 were up-regulated. **Fig. 2B** and **C** show the heatmaps of each heart-

and muscle-specific DE-miRNA identified by NGS. The colors indicate up (red) or down (green) regulation of each DE-miRNA; the brilliance of colors is proportional to the degree of alteration. We also analyzed plasma from PD mice, but we failed to identify DE-miRNAs.

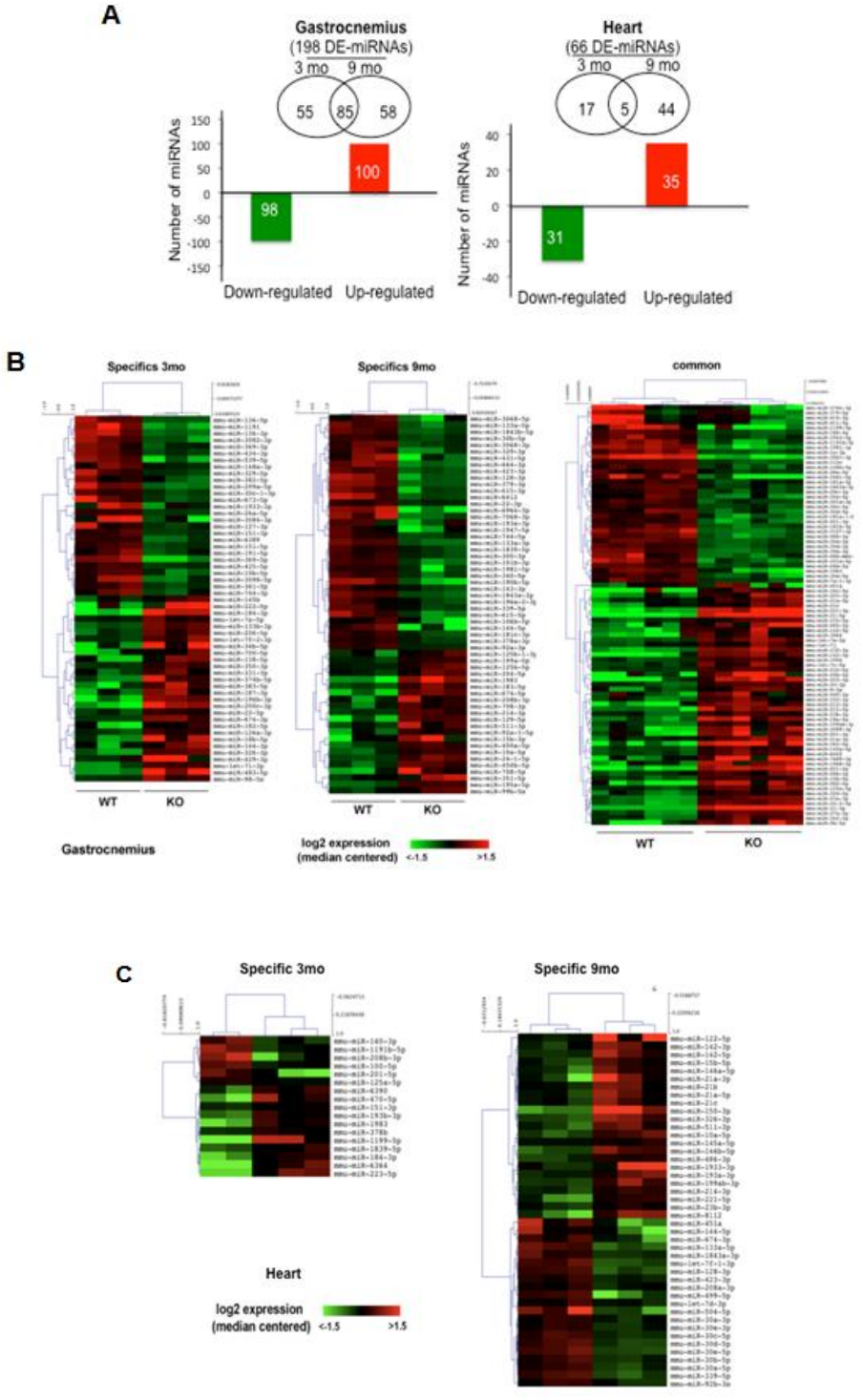


**Fig. 2** miRNAs expression profiles analyzed by NGS in the mouse model of PD in comparison to wild-type animals.

Further analysis was made in order to acquire more information about DE-miRNAs and in order to select DE-miRNAs that were functionally involved in relevant processes for PD. To this aim target genes were predicted using TargetScan and miRDB. Gene Ontology and KEGG pathways analysis were applied to their target pool. As result of KEGG frequencies we found the genes that are predicted to be most frequently targeted by the DE-miRNAs. The most frequent target genes (that is genes that are predicted target at least of 25 DE-miRNAs) are shown in **Fig. 3A**. Among the most frequently targeted genes, some are potentially interesting for PD pathophysiology, while for others the possible link is less obvious.

The predicted target genes of DE-miRNAs are involved in different pathways, including cancer, insulin signaling, diabetes mellitus, and others (**Fig. 3B**). Interestingly, some other pathways are potentially relevant for PD, including mTOR signaling pathway, endocytosis, ubiquitin-mediated proteolysis, calcium signaling. This finding was further supported by the analysis of literature data, indicating that some DE-miRNAs are already known to be implicated in myogenesis, autophagy, cardiac hypertrophy, muscle atrophy, fibrosis.

For example, miR-1 and miR-133, which are co-transcribed, are directly involved in differentiation and proliferation of skeletal muscle during development [12]. The expression of both miR-1 and miR-133 was enriched in striated muscle, including both cardiac and skeletal muscles. In our analysis we found both these miRNAs down-regulated (miR-1 in gastrocnemius, miR-133 in heart and in gastrocnemius). We found the same scenario for others muscular miRNAs; miR-486 has been shown to be upregulated during myogenesis [13], while is down-regulated in PD mouse gastrocnemius; miR-31 and miR-221 have been reported as reduced in myogenesis [14, 15], but in our PD model they were both up-regulated.

A few selected DE-miRNAs and their target genes are shown in **Fig. 3C**. In addition, we found some DE-miRNAs that are implicated in other pathways, such as oxidative stress and inflammation, that have only occasionally been associated with PD, but are of potential interest for the disease pathophysiology.

Some DE-miRNAs are involved in more than one of these pathways, thus providing a picture of the complexity of PD pathophysiology, and of the intricate interplay between secondary cellular events triggered in response to glycogen storage.

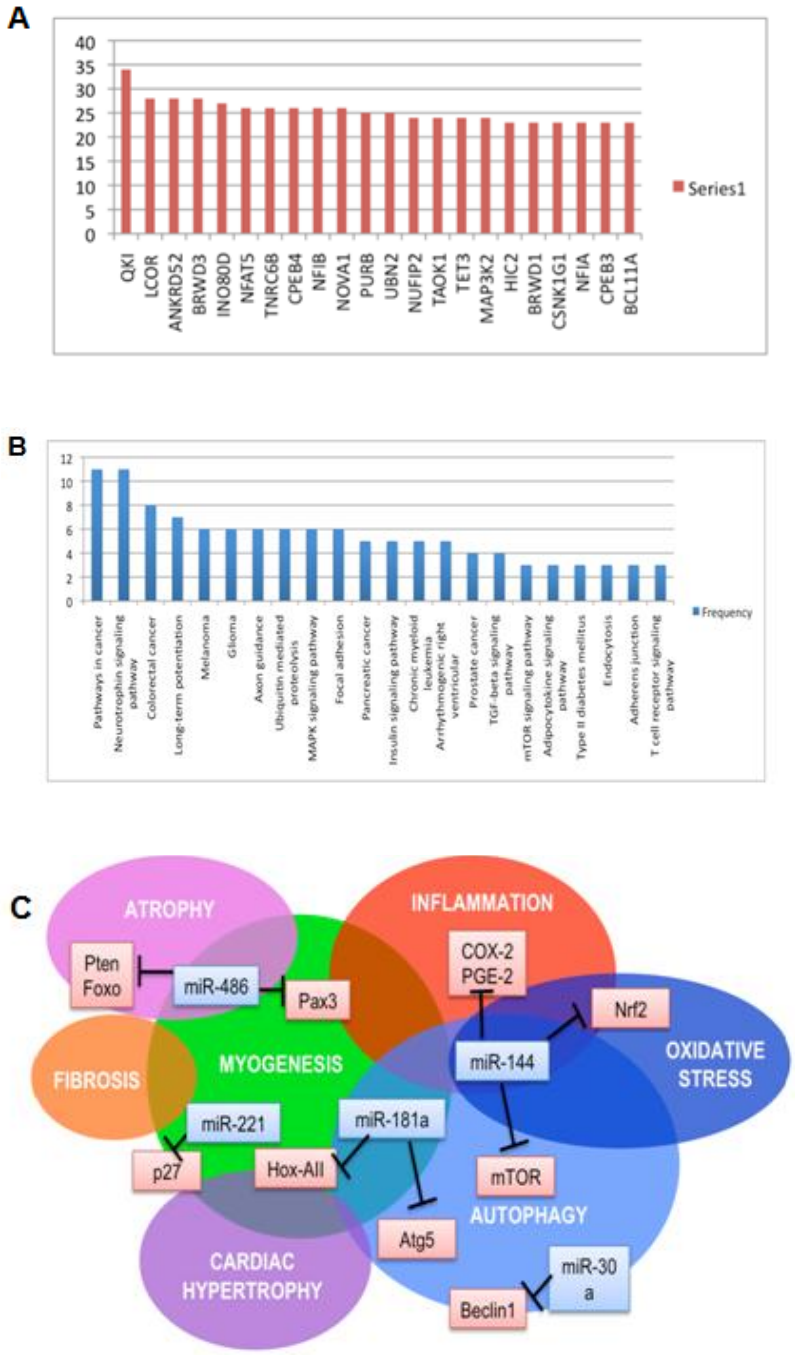


**Fig. 3** PD genes that are predicted to be most frequently targeted by the DE-miRNAs and relevant processes for PD in which DE-miRNAs were functionally involved.

In recent years the role of specific genes in muscle myogenesis, regeneration and atrophy has been widely studied, as well as their regulation by miRNAs [16]. We looked at the expression levels of 3 genes that are relevant for muscle (*FOXO-1*, *Pten*, *Pax7*) and 1 gene involved in autophagy, a pathway that is typically dysregulated in PD

(*Beclin1*) (**Fig. 4**). These genes are known to be regulated by miRNAs that were found to be down-regulated in mice tissues. The analysis was performed by qRT-PCR in mice gastrocnemius.

The Pax family, mainly represented by Pax3 and Pax7, are skeletal muscle progenitor cells markers and critical upstream factors involved in the myogenesis. Pax7 is essential for the specification of skeletal muscle satellite cells, which are skeletal muscle stem cells, as well as for the commitment of the myogenic precursor lineage [17]. FOXO-1 is an important factor in atrophy activation [18]. Pten an essential regulator of SRF-dependent transcription to control smooth muscle differentiation and involved in AKT signaling pathway [19].

Pax7, Foxo1 and Pten are all validated target genes of miR-486. MiR-486 promotes myogenesis and is downregulated in PD mouse gastrocnemius. Beclin1 plays an important role in the autophagic process and is one of the target genes of DE-miRNA miR-30a. All these genes are also target of others DE-miRNAs and their function could be influenced by different factors.

All genes resulted to be up-regulated in gastrocnemius, consistent with the down-regulation of the relevant DE-miRNAs.

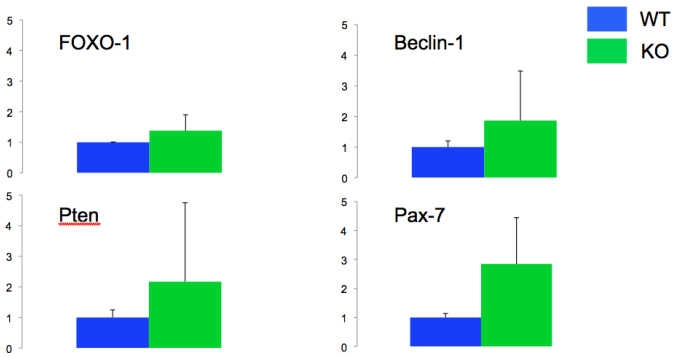


**Fig. 4** Expression levels of FOXO-1, Pten, Pax7 and Beclin 1 analyzed by qRT-PCR in mice gastrocnemius.

- **PD patients show differential expression of circulating miRNAs.**

We then looked at plasma samples from patients affected by PD. Plasma samples from 40 patients, were available at the six clinical centers involved in this study (Università degli Studi di Napoli Federico II, Napoli; Università degli Studi di Messina; Università degli studi di Torino; Ospedale pediatrico Bambin Gesù, Roma; Azienda Ospedaliero Univesitaria Santa Maria della Misericordia di Udine; Erasmus MC: Universitair Medisch Centrum Rotterdam). Eight of the patients were affected by infantile-onset PD (IOPD), 32 by late-onset PD (LOPD).

Six plasma samples of them were selected for NGS analysis, with the same approach used in mice tissues. The patients to be analyzed were selected based on their phenotype, current clinical condition and age, in order have homogeneous groups representative of both PD patients categories, IOPD and LOPD. The results obtained in IOPD patients were compared with those obtained in six controls (3 infants, 3 age-matched adults, see above).

We found 55 miRNAs that were significant dysregulated in PD samples with respect to controls (28 down-regulated and 27 up-regulated) (**Fig. 5A**).

A comparison between the results obtained in mice and those obtained in patients plasma showed that 19 miRNAs were differentially expressed both in tissues from the PD mouse and in patients plasma. 15 miRNAs were differentially expressed in mouse gastrocnemius and plasma, 3 in heart and plasma, one was differentially expressed in all samples examined (**Fig. 5B**).

Interestingly mir-29c was found to be altered both in tissues of animal model and in plasma of PD patients. This miRNA is involved in different relevant process as cancer, Alzheimer's disease, cardiomyopathies. miR-29c showed a distinct signature in aortic

stenosis, hypertrophic non-obstructive and obstructive cardiomyopathies and thus could be developed into a clinically useful biomarker [20].

MiR-133 has been already proposed (together with other miRNAs) as new and valuable biomarkers for the diagnosis of Duchenne muscular distrophy [10] and possibly for monitoring the outcomes of therapeutic interventions in humans. In our analysis miR-133 was dysregulated in plasma from PD patients and in mice gastrocnemius.

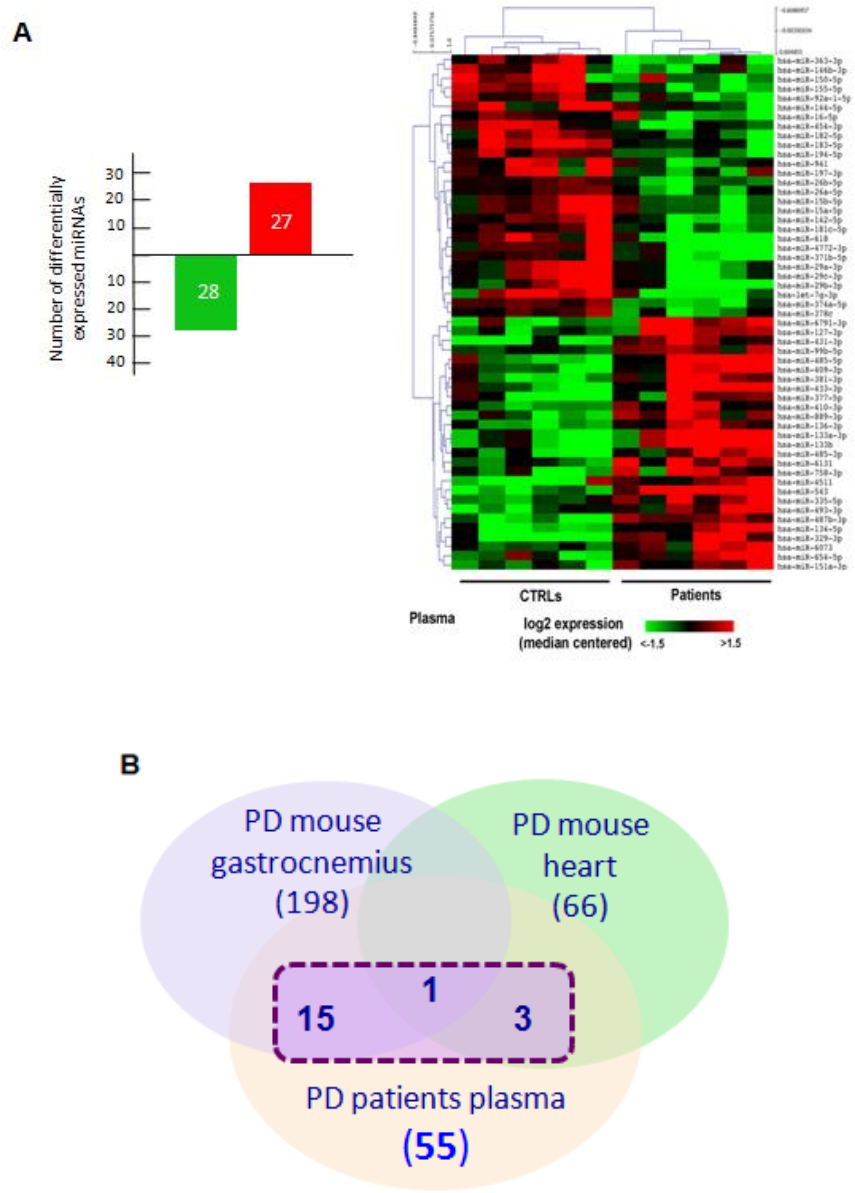


**Fig. 5** NGS analysis of plasma samples from patients affected by PD

**Fig. 6** shows the results of selected miRNAs that were significant dysregulated in PD samples with respect to controls and that are involved in pathway such as autophagy, inflammation, muscle regeneration and atrophy. miR-133, -134 and -136 resulted to be up-regulated in PD samples, instead of miR-155 and miR-142 that resulted down-regulated in PD patients. All these miRNAs were dysregulated with high statistical significance (0,002 ≤ p ≤ 0,01). For some of them minor overlap between PD and control plasma was detectable. When we considered mi-RNA 155/136 ratio, the differences in expression levels between PD and controls became even more significant (we used a logarithmic scale).

We then looked for a pattern of miRNA expression that may rapresent a “signature” of PD and a tool to monitor disease progression and the effects of therapies.

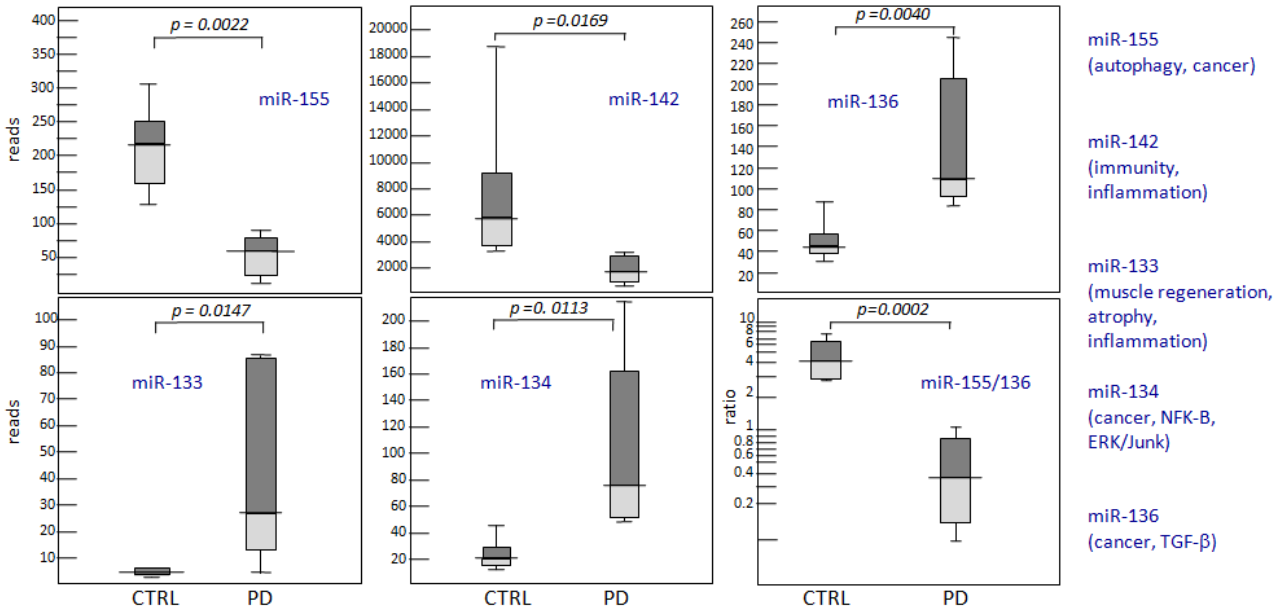


**Fig. 6**Plasma level of some of miRNAs in PD samples with respect to controls

**METHODS**

A KO Pompe disease mouse model obtained by insertion of neo into the *GAA* gene exon 6 Raben et al, [1998] was purchased from Charles River Laboratories (Wilmington, MA), and is currently maintained at the Cardarelli Hospital's Animal Facility (Naples, Italy).Animal studies were performed according to the EU Directive 86/609, regarding the protection of animals used for experimental purposes. Every procedure on the mice were performed with the aim of ensuring that discomfort, distress, pain, and injury would be minimal. Mice were euthanized following ketamine xylazine anesthesia.

Human PD fibroblasts (approximately 30 cell lines) and myoblasts (5 cell lines) are already available at the cell bank of the Department of Translational Medical Sciences (DISMET), Section of Pediatrics,Federico II University, Naples. Plasma samples were collected from 40 PD patients in 7 collaborating centers (DISMET and Department of Neurosciences, Federico II University in Naples, University of Messina, Bambino Gesù Hospital in Rome, Centre for Rare Disease, Udine, at Department of Neurosciences, University of Turin and at Center for Lysosomal and Metabolic Diseases and at Department of Pediatrics, Erasmus University Medical Center, Rotterdam, The Netherlands). Plasma was obtained according to standard procedures during periodic follow-up admissions to the respective Hospital. Five ml of peripheral blood was collected in EDTA and immediately processed, or stored at -80°C. Samples from age-matched controls were analyzed for comparison.

Nine muscle biopsy samples are already available at DISMET (kindly provided by Prof. Antonio Toscano, Dept. of Neurology, University of Messina, and by Prof. Lucio Santoro, Dept. of Neurosciences, Federico II University, Naples). The samples have been obtained for diagnostic purposes and patients have consented to their storage and use for research.

*Total RNA extraction preserving miRNA fraction.*

The methodology for extraction and analysis is already established in our laboratories. Tissue samples were immediately submerged in RNA Stabilization Reagent (RNA later; QIAGEN), to stabilize RNA and preserve the gene expression profile, and frozen. Total RNA, including small RNAs, was extracted using the miRNeasy Kit (Qiagen) following the manufacturer's instructions. RNA was quantified using a NanoDrop ND-8000 spectrophotometer (NanoDrop Technologies) and the integrity was evaluated using an RNA 6000 Nano chip on a Bioanalyzer (Agilent Technologies). Only samples with an RNA integrity number (RIN)>8.0 were used for library preparation.

*Small RNA-seq analysis in tissues*

Small RNA libraries were constructed using a Truseq small RNA sample preparation kit (Illumina) following the manufacturer's protocol. Using multiplexing, we combined up to 12 samples into a single lane in order to obtain sufficient coverage. Equal volumes of the samples that constituted each library were pooled together immediately prior to gel purification and the 147-157 bp products from the pooled indexes were purified from a 6% polyacrylamide gel (Invitrogen). Libraries have been quality-checked using a DNA 1000 chip on a Bioanalyzer (Agilent Technologies) and quantified using the Qubit® 2.0 Fluorometer (Invitrogen).

*Small RNA-seq analysis in plasma*

For the analysis of circulating miRNA, we collected plasma from PD mice and age-matched wild-type mice by centrifugation of blood in serological tubes. For the preparation of plasma, EDTA was used as anticoagulant. Every effort was made to limit pre-analytical variation that could affect miRNA quantification. For instance, particular attention was given to prevent hemolysis. We monitored the levels of the granulocyte-

specific miR-223 to assess the extent of hemolysis in the collected samples. All downstream processing of plasma samples from PD and control sets were conducted simultaneously to minimize batch effect. Prior to RNA extraction, a C. elegans-specific synthetic exogenous miRNA (ce-miR-39) was spiked in the samples as control for the extraction efficiency. RNA was isolated using the miRNeasy Kit (Qiagen) and RT-PCR was performed using miScript System (Qiagen). RNA recovery was assessed by comparing the Ct values (obtained with the assay targeting the synthetic miRNA) with a standard curve of the synthetic miRNA generated independently of the RNA purification procedure. After the assessment of RNA recovery, equal amounts based on starting volume (3 □l) were used for the preparation of small RNA libraries, as previously described for tissue samples.

The sequencing was carried out by the NGS Core Facility at TIGEM, Naples. Cluster generation was performed on a Flow Cell v3 (TruSeq SR Cluster Kit v3; Illumina) using cBOT and sequencing was performed on the Illumina HiSeq1000 platform, according to the manufacturer's protocol. Each library was loaded at a concentration of 10 pM, which we had previously established as optimal.

*Bioinformatics Analysis*

To identify differentially expressed miRNAs (DE-miRNAs) across samples, the raw data were analyzed with the support of the Bioinformatics and Statistics Core Facility, TIGEM, Naples. Briefly, the reads were trimmed to remove adapter sequences and low quality ends, and reads mapping to contaminating sequences (e.g. ribosomal RNA, phIX control) were filtered-out. The filtered reads were aligned in parallel both to the mouse genome (mm10) and to mouse mature miRNAs (miRBase Release 20) using the CASAVA software (Illumina). The number of reads for each miRNA was normalised

using Trimmed Mean of MS (TMM). The comparative analysis of miRNA levels across samples was performed with edgeR, a statistical package based on generalized linear models, suitable for multifactorial experiments.

The potential role, the target genes, and the pathways in which DE-miRNA identified by NGS were involved, were studied by bioinformatics tools (Gene Ontology, KEGG frequencies) and literature-based analysis (PubMed).

*Quantitative Real-time Reverse-transcription Polymerase Chain Reaction (qRT-PCR) of miRNA and of specific target genes.*

Expression of mature miRNAs were assayed using Taqman MicroRNA Assay (Applied Biosystems) specific for each miRNA selected for validation. qRT-PCR was performed by using an Applied Biosystems 7900 Real-time PCR System and a TaqMan Universal PCR Master Mix. All the primers for selected miRNAs were obtained from the TaqMan miRNA Assays. Samples were run in triplicate and small nuclear U6 snRNA and miR-16 (Applied Biosystems) were used as internal controls.

Differences in miRNAs expression, expressed as fold-changes, were calculated using the 2-DDCt method. To validate the target genes expression data, qRT-PCR was performed for selected target genes of some miRNAs. GAPDH, was used as endogenous reference transcript. The levels of selected target genes were measured by qRT-PCR using the LightCycler 480 (Roche) and specific forward and reverse primers for each target gene. The PCRs with cDNA were carried out in a total volume of 20 µl, using 10 µl LightCycler 480 SYBR Green I Master Mix (Roche) and 400nM specific primers under specific conditions that were validated for each of the genes analyzed. All the reactions were normalized against murine or human GAPDH. Each sample was analyzed in duplicate in two-independent experiments.

*In vivo experiments on PD mouse model*

PD ko mice received single injection of Myozyme into the retro-orbital vein (doses: 40 mg/kg; 100 mg/kg). The dose of 40 mg/kg corresponds to the dose used in human therapy. Plasma and tissue (heart, gastrocnemius) were collected 24 hrs or 48 hrs after the infusion and selected miRNA and mRNAs were analyzed by qRT-PCR as indicated. The results were compared with those obtained in untreated animals. For each group (treated, untreated, different time points) 5 animals were tested.

Plasma was obtained according to standard procedures during periodic follow-up admissions to the respective Hospitals. Peripheral blood was collected in EDTA and immediately processed, or stored at -80°C. Samples from age-matched controls were analyzed for comparison.

RNA was extracted (as described) and analyzed by qRT-PCR as indicated above.

*Patients*

Forty PD patients were recruited for the study. The patients were followed at six Italian centers and one Dutch center (Department of TranslationalMedicine, Federico II University of Naples, Department of Neurosciences, Federico II University of Naples, University of Messina, Bambino Gesù Hospital of Rome, Centre for Rare Disease of Udine, Department of Neurosciences, University of Turin and Center for Lysosomal and Metabolic Diseases and Department of Pediatrics, Erasmus University Medical Center, Rotterdam, The Netherlands). All these Institutions are referral centers for the diagnosis, care and follow-up of inborn errors of metabolism. In all patients, the clinical and enzymatic diagnosis was confirmed by the molecular analysis of the *GAA* gene. Each patient ID is composed by initials of the city center + progressive number.

Plasma was obtained according to standard procedures during periodic follow-up admissions to the respective Hospital. Patients (or their legal guardians) signed an informed consent agreeing that samples obtained would be stored and used for the study purposes and for possible future research purposes.

## CONCLUSIONS

The availability of objective, reliable and reproducible tests is important to assess disease progression and to monitor efficacy of therapies in PD patients. Currently, like in many other myopathies, most of the indicators of PD rely on clinical tests or patient-reported outcome measures, with only a few based on biochemical assays.

We have evaluated miRNAs as potential biomarkers for PD. We initially performed our analysis in the murine model of the disease in order to start with a homogenous sample, with a common genetic background and uniform disease progression. PD patients are highly heterogeneous with respect to phenotype, disease course, response to ERT, and appeared to be not appropriate for the initial screening of DE-miRNAs. In addition, the use of the murine model of the disease allowed for analysis of tissues, that in patients would require invasive procedures. We studied miRNAs profiles in tissues from PD mice at two stages of disease progression, 3 and 9 months. We used an approach based on next generation sequencing (NGS), a powerful and innovative tool that allows large-scale quantitative analysis of genes and nucleotide sequences. The NGS-by-synthesis approach allows for detection of even small differences among samples, and enables the identification of non-annotated miRNAs. In addition, the NGS-by-synthesis approach allows for detection of even small differences among samples, and enables the identification of non-annotated miRNAs.

We identified 198 miRNA that were differentially expressed with statistical significance (FDR< 0.05) in muscle (gastrocnemius), and 66 in heart. In total, 72 miRNAs were differentially expressed at 3 months, 102 at 9 months, 90 were differentially expressed at both ages.

Interestingly, some of these miRNAs are already known to modulate the expression of genes involved in pathways such as autophagy, muscle regeneration, inflammation that may be relevant for PD pathophysiology. This supports the value of our analysis.

In patients we performed NGS analysis, with the same approach used in mice tissues. Expression levels of all 55 DE-miRNAs found by NGS analysis in control and PD plasma samples will be further evaluated.

This research has the potential to generate reliable tools for PD that can be used in clinics to monitor disease progression and ERT efficacy, to provide information on the disease pathophysiology, and to help optimize therapeutic interventions.

## BIBLIOGRAPHY

[1] Vill K, Schessl J, Teusch V, Schroeder S, Blaschek A, Schoser B, Muller-Felber W. Muscle ultrasound in classic infantile and adult Pompe disease: A useful screening tool in adults but not in infants. Neuromuscul Disord. 2014 Oct 22. pii: S0960-8966(14)00662-2

[2] Angelini C, Semplicini C, Ravaglia S, Moggio M, Comi GP, Musumeci O, Pegoraro E, Tonin P, Filosto M, Servidei S, Morandi L, Crescimanno G, Marrosu G, Siciliano G, Mongini T, Toscano A; Italian Group on GSDII. New motor outcome function measures in evaluation of late-onset Pompe disease before and after enzyme replacement therapy. Muscle Nerve. 2012 Jun;45(6):831-4

[3] van der Beek NA, de Vries JM, Hagemans ML, Hop WC, Kroos MA, Wokke JH, de Visser M, van Engelen BG, Kuks JB, van der Kooi AJ, Notermans NC, Faber KG, Verschuuren JJ, Reuser AJ, van der Ploeg AT, van Doorn PA. Clinical features and predictors for disease natural progression in adults with Pompe disease: a nationwide prospective observational study. Orphanet J Rare Dis. 2012 Nov 12;7:88

[4] Young SP, Zhang H, Corzo D, Thurberg BL, Bali D, Kishnani PS, Millington DS. Long-term monitoring of patients with infantile-onset Pompe disease on enzyme replacement therapy using a urinary glucose tetrasaccharide biomarker. Genet Med. 2009 Jul;11(7):536-41

[5] Vill K, Schessl J, Teusch V, Schroeder S, Blaschek A, Schoser B, Muller-Felber W. Muscle ultrasound in classic infantile and adult Pompe disease: A useful screening tool in adults but not in infants. Neuromuscul Disord. 2014 Oct 22. pii: S0960-8966(14)00662-2

[6] Mercuri, E, Pichiecchio, A, Counsell, S, Allsop, J, Cini, C, Jungbluth, H et al.. A short protocol for muscle MRI in children with muscular dystrophies. Eur J Paediat Neurol 6: 305-307. (2002)

[7] Bushati N, Cohen SM: microRNA functions. Annual review of cell and developmental biology 2007, 23:175-205.

[8] Bartel DP: MicroRNAs: target recognition and regulatory functions. Cell 2009, 136(2):215-233.

[9] Pasquinelli AE: MicroRNAs and their targets: recognition, regulation and an emerging reciprocal relationship. Nature reviews Genetics 2012, 13(4):271-282.

[10] Cacchiarelli D, Legnini I, Martone J, Cazzella V, D'Amico A, Bertini E, Bozzoni I: miRNAs as serum biomarkers for Duchenne muscular dystrophy. EMBO molecular medicine 2011, 3(5):258-265.

[11] Allegra A, Alonci A, Campo S, Penna G, Petrungaro A, Gerace D, Musolino C: Circulating microRNAs: new biomarkers in diagnosis, prognosis and treatment of cancer (review). International journal of oncology 2012, 41(6):1897-1912.

[12] Cheng Y, Tan N, Yang J, Liu X, Cao X, He P, Dong X, Qin S, Zhang C: A translational study of circulating cell-free microRNA-1 in acute myocardial infarction. Clinical science 2010, 119(2):87-95.

[13] Dey BK1, Gagan J, Dutta A. miR-206 and -486 induce myoblast differentiation by downregulating Pax7. Mol Cell Biol. 2011 Jan;31(1):203-14. doi: 10.1128/MCB.01009-10. Epub 2010 Nov 1.

[14] Crist CG1, Montarras D, Buckingham M. Muscle satellite cells are primed for myogenesis but maintain quiescence with sequestration of Myf5 mRNA targeted by microRNA-31 in mRNP granules. Cell Stem Cell. 2012 Jul 6;11(1):118-26.

[15] Cardinali B1, Castellani L, Fasanaro P, Basso A, Alemà S, Martelli F, Falcone G. Microrna-221 and microrna-222 modulate differentiation and maturation of skeletal muscle cells. PLoS One. 2009 Oct 27;4(10):e7607.

[16] Diniz GP, Wang DZ. Regulation of Skeletal Muscle by microRNAs. Compr Physiol. 2016 Jun 13;6(3):1279-94.

[17] Buckingham M, Relaix F. PAX3 and PAX7 as upstream regulators of myogenesis. Semin Cell Dev Biol. 2015 Aug;44:115-25.

[18] Seiliez I1, Sabin N, Gabillard JC. FoxO1 is not a key transcription factor in the regulation of myostatin (mstn-1a and mstn-1b) gene expression in trout myotubes. Am J Physiol Regul Integr Comp Physiol. 2011 Jul;301(1):R97-104.

[19] Small EM1, O'Rourke JR, Moresi V, Sutherland LB, McAnally J, Gerard RD, Richardson JA, Olson EN. Regulation of PI3-kinase/Akt signaling by muscle-enriched microRNA-486. Proc Natl Acad Sci U S A. 2010 Mar 2;107(9):4218-23.

[20] Zong Y, Yu P, Cheng H, Wang H, Wang X, Liang C, Zhu H, Qin Y, Qin C. miR-29c regulates NAV3 protein expression in a transgenic mouse model of Alzheimer's disease. Brain Res. 2015 Oct 22;1624:95-102.

## GENERAL CONCLUSION

PD phenotype, biochemical and molecular basis have been fully characterized. A treatment, ERT, has been developed and approved in 2006, with remarkable success in prolonging patients survival and improving motor and respiratory functions.

Nevertheless, many aspects of PD pathophysiology remain elusive. In addition ERT has limited efficacy, indeed not all patients respond equally well to treatment and skeletal muscle is more refractory to treatment than other tissues; moreover the evaluation of its efficacy is difficult.

Current issues that deserve future investigation in PD are:

- Need for full understanding of the disease pathophysiology
- Identification of additional therapeutic targets and strategies to improve the efficacy of ERT
- Identification of novel markers of disease progression and efficacy of therapies.

The scope of the present work was to address these issues.We have investigated:

a) GAA interactions

b) Ox-stress in PD

c) miRNAs as biomarkers in PD

a) **Interaction of GAA with GSN**. The role of this interaction is not clear. Perhaps it is involved in the (early) trafficking of GAA or of both proteins. However, this indicates that there is much to learn about the pathophysiology of PD. A complete understanding of these processes may open the way to the discovery of new therapeutic targets.

b) **Ox-stress in PD**. The derangement of secondary pathways is emerging as an important factor in many LSDs, including PD. In PD autophagy is known to be altered and a close interaction between autophagy and ox-stress has been shown. In addition, it has been found that PD mice and humans show multiple mitochondrial defects, a profound dysregulation of Ca2+ homeostasis and an increase in reactive oxygen species.

We have provided several lines of evidence supporting the presence of increased ox-stress in PD, both in vitro (fibros from patients) and in vivo, in the PD mouse model. Ox-stress may become a novel therapeutic target and can be decreased by using known drugs. It may impact on the efficacy of therapies, such as ERT; indeed, when we have treated KO mice and PD fibroblasts with C002, we observed a significant improvement of rhGAA activity.

We have tested few antioxidant drugs derived from literature analysis but we may test more drugs.Therefore experiments *in vitro* may be a useful tool, that may be pharmacologically manipulated and then tested *in vivo*, in mouse model, for the functional effects.

c) **miRNAs as biomarkers in PD**. Assessing patient conditions and response to ERT is a critical issue in the management of PD. A major challenge, in this respect, is the need for reliable, measurable and objective markers of disease. In our work we found:

- 198 miRNAs differentially expressed with statistical significance in gastrocnemius and 66 DE-miRNAs in heart in mouse model

- 55 miRNAs differentially expressed in patients' plasma.

It was an expected result to find more DE-miRNAs in tissue and less in plasma. De-miRNAs found in plasma are involved in processes and pathways that are known to be relevant for PD.

Obviously, it is necessary to perform more studies on large cohorts of patients to establish possible correlations between miRNAs and ERT or disease progression.